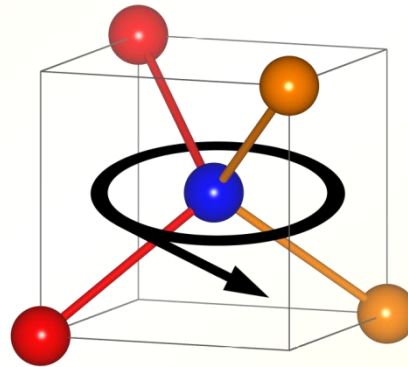


X-ray absorption spectroscopy and its application to chalcopyrite and kesterite materials



Claudia S. Schnohr

Institut für Festkörperphysik, Friedrich-Schiller-Universität Jena, Germany

Part I Basics of XAS

Part II Experimental aspects of XAS

Part III Applications of XAS to chalcopyrite and kesterite materials

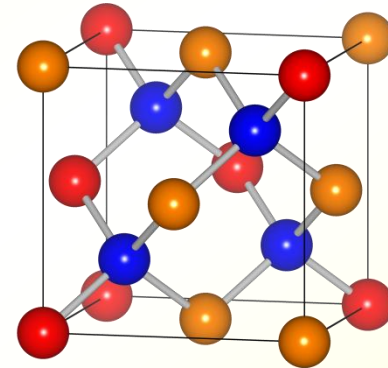
X-ray absorption spectroscopy (XAS)

powerful technique for structural analysis

complementary to other techniques
such as diffraction or electron microscopy

applicable to crystalline and disordered materials,
liquids and even gases

physics, chemistry, material science, geology,
biology, environmental science, ...



Literature

Books

S. Calvin, *XAFS for Everyone*, CRC Press, 2013

G. Bunker, *Introduction to XAFS*, Cambridge University Press, 2010

S. D. Kelly et al., *Analysis of Soils and Minerals Using X-ray Absorption Spectroscopy*, Book Chapter, Soil Science Society of America Book Series No. 5, 2008

C.S. Schnohr, M.C. Ridgway, *X-ray Absorption Spectroscopy of Semiconductors*, Springer, 2015

Internet

<http://www.ixasportal.net/ixas/>

→ <http://www.ixasportal.net/wiki/doku.php>

<http://xafs.org/>



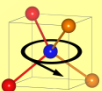
Contents – Part I

Basic principle

XANES

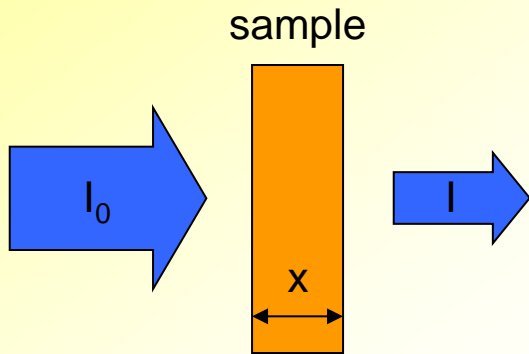
EXAFS

Summary

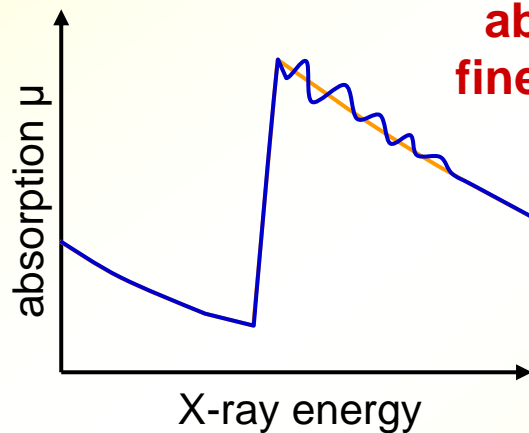


Basic principle

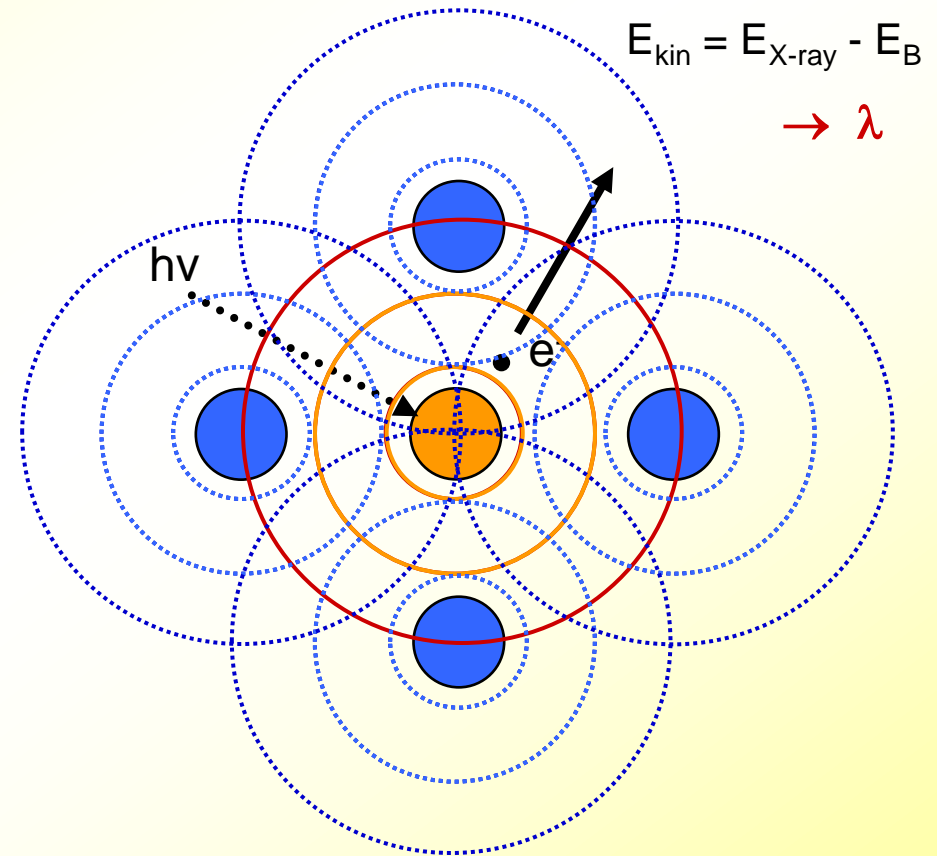
X-ray absorption



$$I = I_0 e^{-\mu x}$$



**X-ray
absorption
fine structure
(XAFS)**

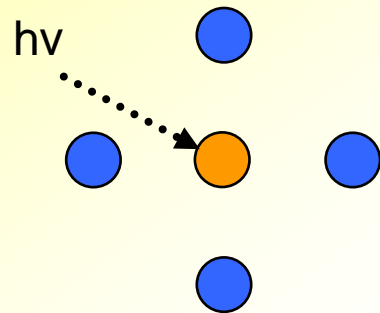


final state → superposition of
outgoing and scattered waves

Basic principle

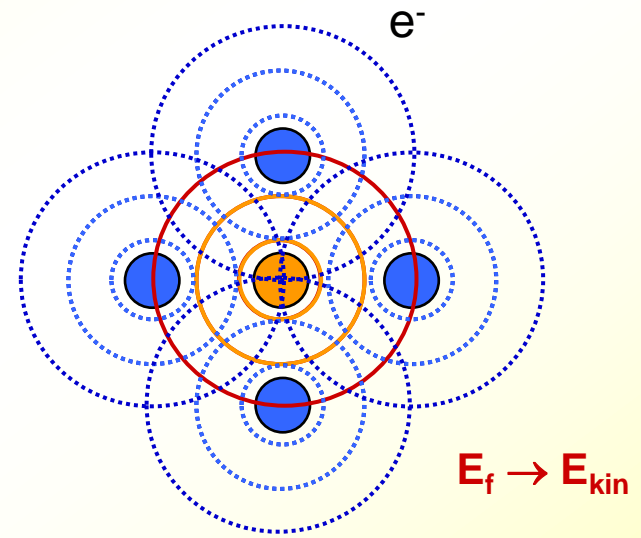
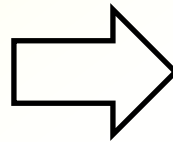
Fermi's Golden Rule

quantum mechanics



initial state i

transition



final state f

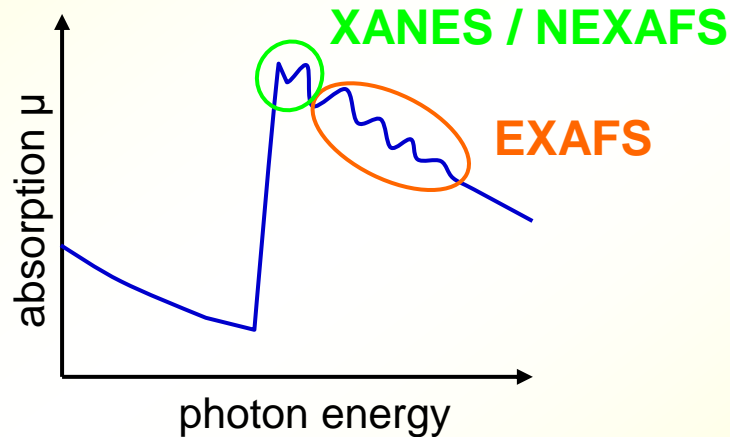
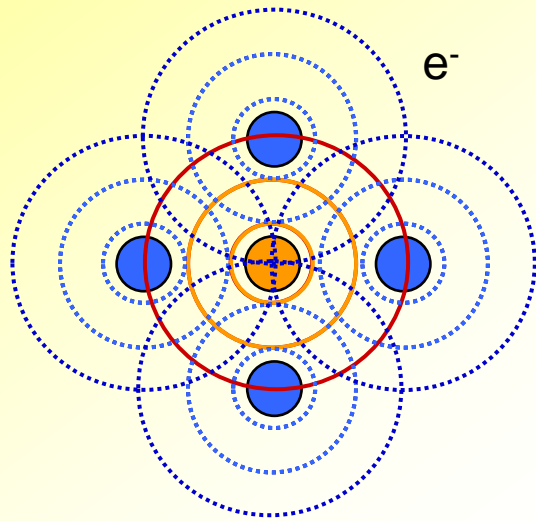
transition probability:

$$\mu \propto \underbrace{|\langle f | H_{X-ray} | i \rangle|^2}_{\text{matrix element } M_{if}} \underbrace{\rho(E_f)}_{\text{density of states}}$$



Basic principle

Characteristics of XAS



fine structure of a particular absorption edge

→ **element-specific**

short range probe ($\sim 10 \text{ \AA}$)

→ **no long-range order needed**

instantaneous configuration around the absorber

→ **correlated motion**

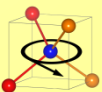
Contents – Part I

Basic principle ✓

XANES

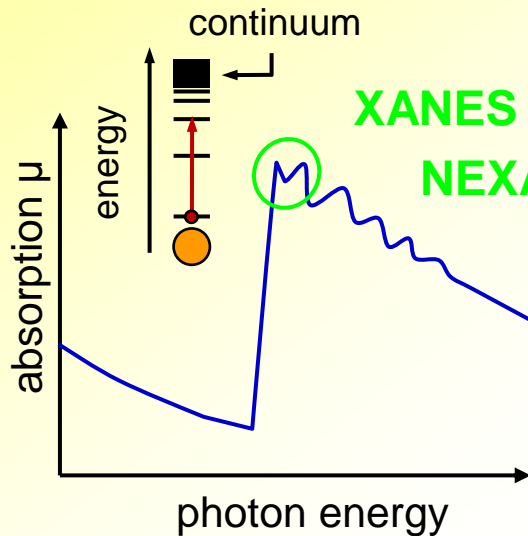
EXAFS

Summary



XANES

Characteristics



XANES ... X-ray Absorption Near Edge Structure

NEXAFS ... Near Edge X-ray Absorption Fine Structure

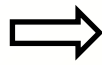
$$\mu \propto \underbrace{|\langle f | H_{X\text{-ray}} | i \rangle|^2}_{\text{matrix element } M_{if}} \underbrace{\rho(E_f)}_{\text{density of states}}$$

$\rho(E_f)$

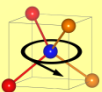


excitation to unoccupied bound states
→ **density of states, chemical bonding**
dipole transition → selection rules

M_{if}



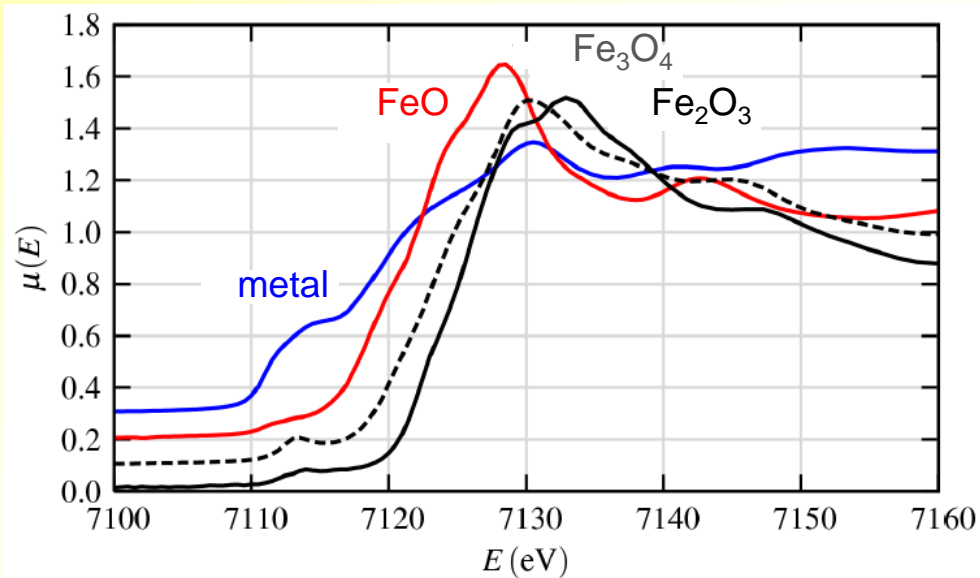
multiple scattering effects
→ **crystal or cluster symmetry**



XANES

Chemical bonding

Fe K-edge of Fe oxides and Fe metal

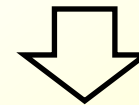


Newville, Fundamentals of XAFS
www.xafs.org/Tutorials

valence state of the
absorber

&

number and kind of
nearest neighbours



position and shape
of edge region

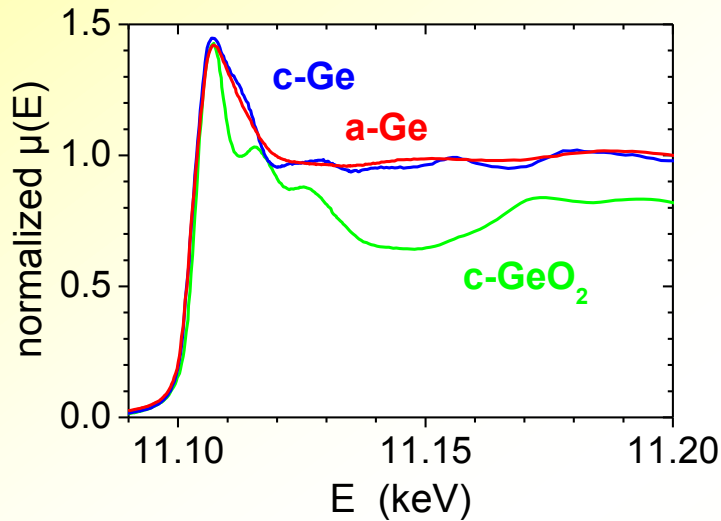
XANES → density of states, chemical bonding, valence state

XANES

Structure

Ge K-edge of Ge

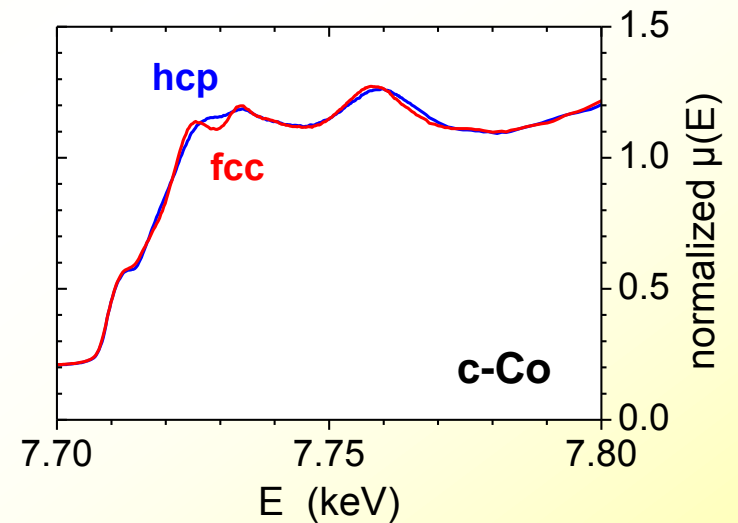
crystalline vs. amorphous



Araujo et al., PRB 78, 2008

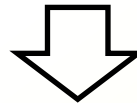
Co K-edge of Co

hcp vs. fcc



Sprouster et al., PRB 80, 2009

structure
&
symmetry



shape of
edge region

XANES → crystal or cluster symmetry



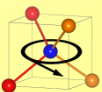
Contents – Part I

Basic principle ✓

XANES ✓

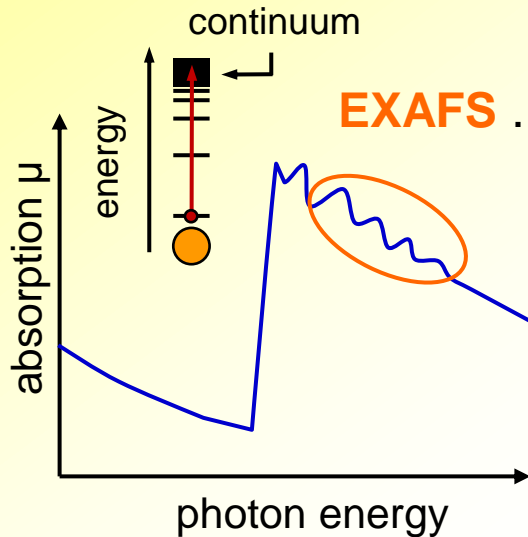
EXAFS

Summary



EXAFS

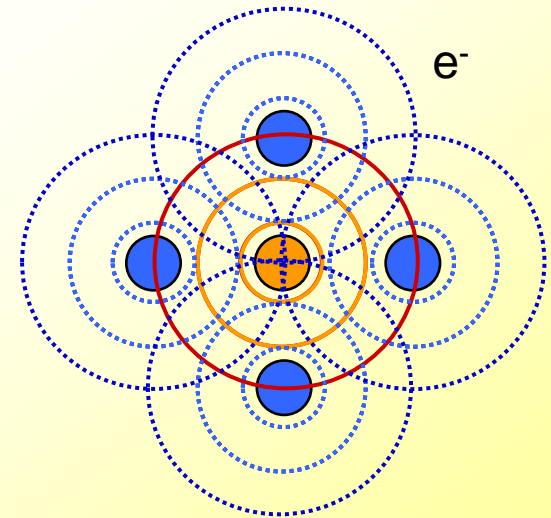
Characteristics



EXAFS ... Extended X-ray Absorption Fine Structure
~ 30 ... 1000 eV above the edge

$$\mu \propto \underbrace{|\langle f | H_{X-ray} | i \rangle|^2}_{\text{matrix element } M_{if}} \underbrace{\rho(E_f)}_{\text{density of states}}$$

M_{if} \Rightarrow structural environment of absorber
 \rightarrow **coordination number,**
bond lengths,
disorder,
...

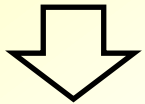


EXAFS

Structural parameters

EXAFS measures instantaneous configuration
thermal vibrations & static disorder

→ **distance distribution**



parameters

mean value (d)

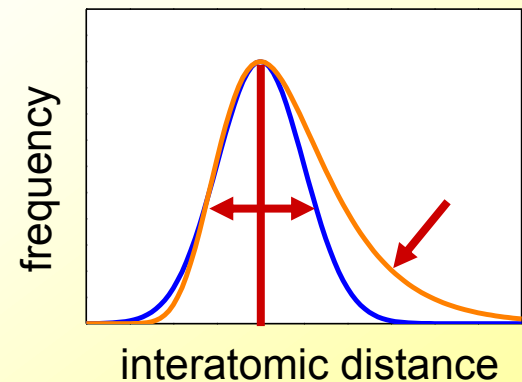
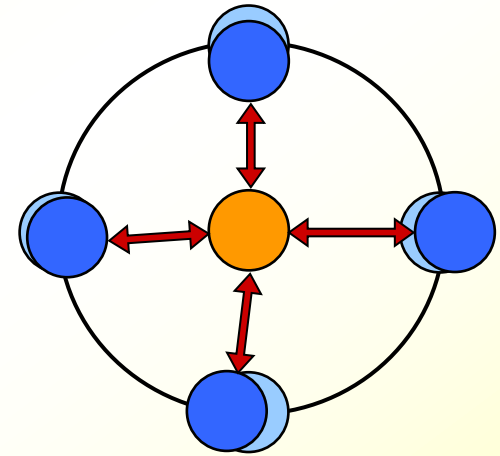
→ **average distance, i.e. bond length**

standard deviation (σ)

→ **variation of distances**

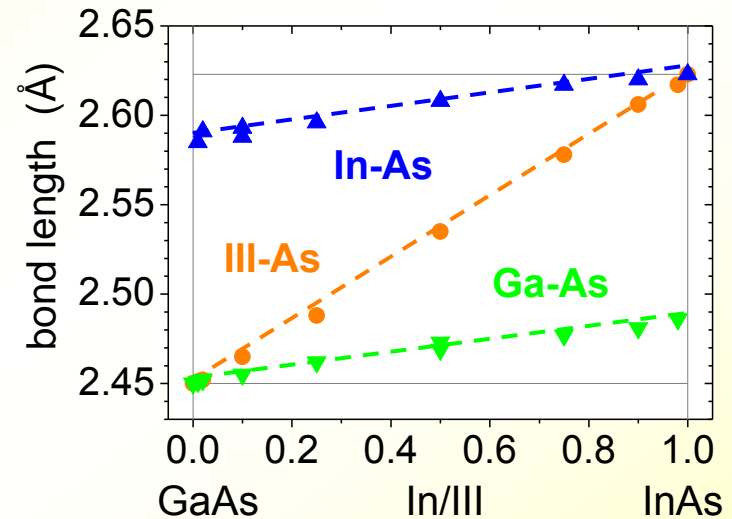
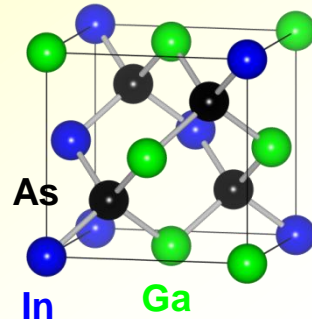
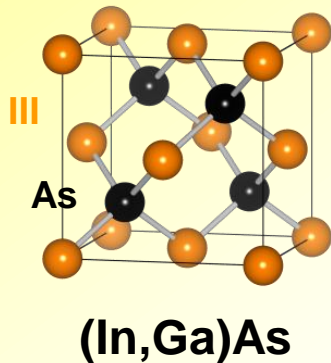
asymmetry (C3)

→ **excess of shorter or longer distances**



EXAFS

Bond lengths



Mikkelsen & Boyce, PRL 49, 1982

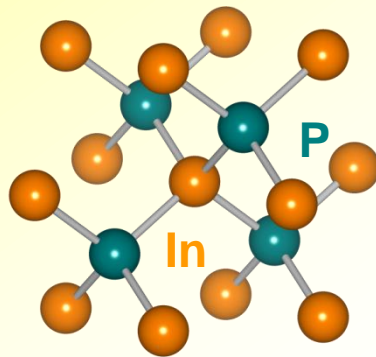
- In-As and Ga-As bond lengths are very different from average III-As distance
- local atomic arrangements deviate from crystallographic structure

EXAFS → element-specific bond lengths

EXAFS

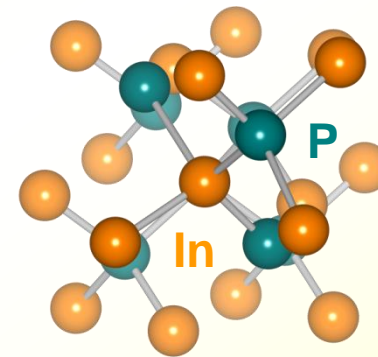
Coordination number and disorder

crystalline InP



*Schnohr et al.,
PRB 77, 2008
PRB 79, 2009*

amorphous InP



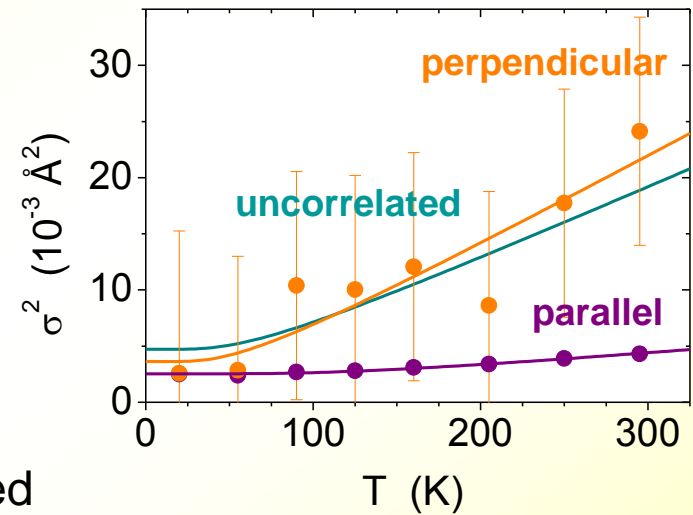
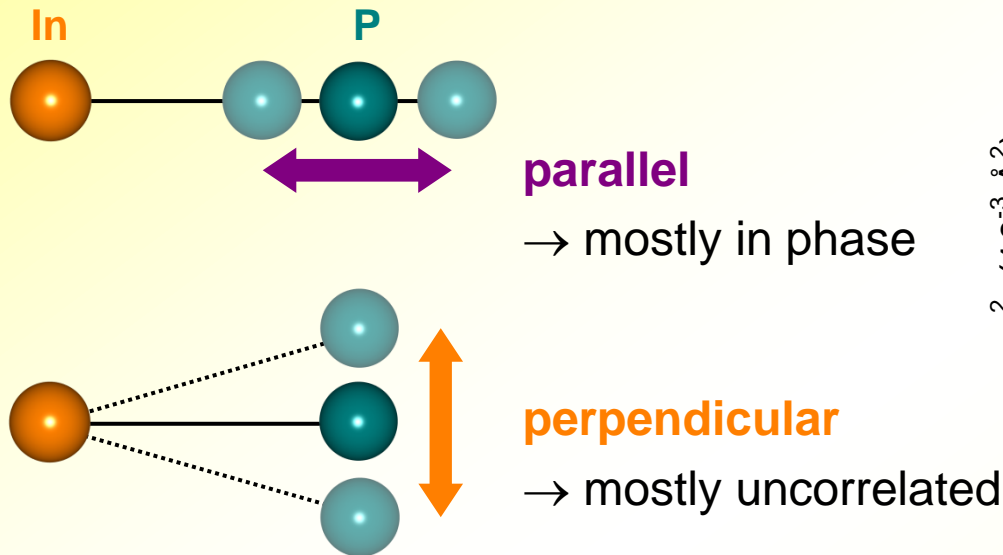
structural parameters

4	N	3.4 (3)	0.7 (3)
2.541 (5)	d (Å)	2.584 (3)	2.799 (6)
2.5 (2)	σ^2 (10^{-3} \AA^2)	5.6 (2)	5.8 (2)
0	C3 (10^{-5} \AA^3)	22 (7)	10 (20)

EXAFS → structural parameters of crystalline and disordered materials

EXAFS

Atomic vibrations



Schnohr et al., PRB 79, 2009

→ bond stretching requires more energy than bond bending

→ force constants for correlated motion

EXAFS → relative vibrations of neighbouring atoms

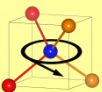
Contents – Part I

Basic principle ✓

XANES ✓

EXAFS ✓

Summary



Summary

X-ray absorption spectroscopy (XAS)

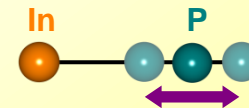
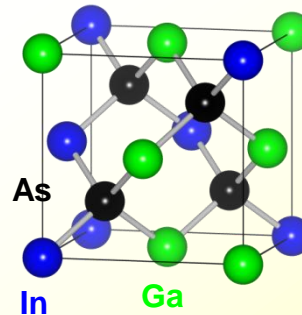
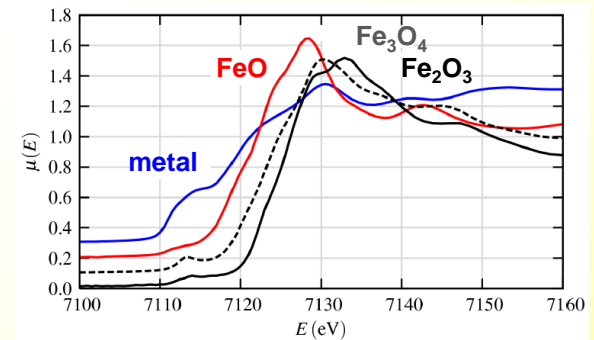
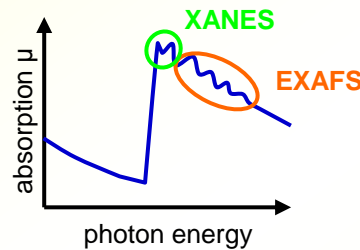
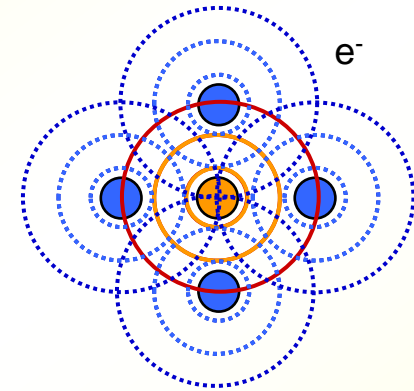
- structural analysis on sub-nm scale
- crystalline and disordered solids, liquids, ...
- element-specific

XANES

- density of states, chemical bonding
- crystal or cluster symmetry

EXAFS

- coordination number
- bond lengths
- static disorder
- atomic vibrations



Part I Basics of XAS

Part II Experimental aspects of XAS

Part III Applications of XAS to chalcopyrite and kesterite materials

Contents – Part II

X-ray sources

Experimental techniques

Sample preparation

Data analysis

XANES

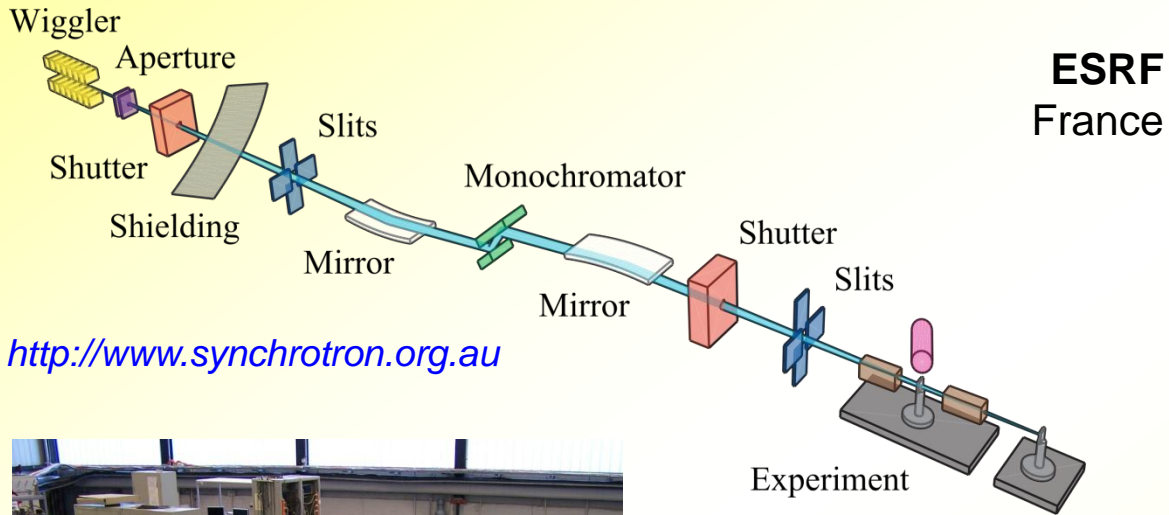
EXAFS

Summary



X-ray sources

XAS beamlines



<http://www.synchrotron.org.au>



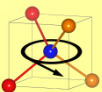
DESY
Hamburg



ESRF
France



SLS
Switzerland



Contents – Part II

X-ray sources ✓

Experimental techniques

Sample preparation

Data analysis

XANES

EXAFS

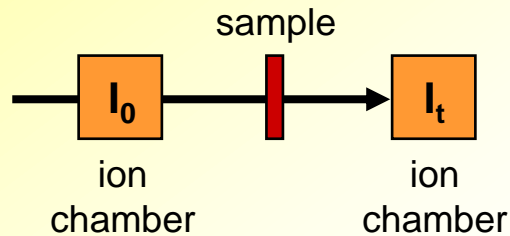
Summary



Experimental techniques

Detection modes

Transmission



→ bulk sensitive

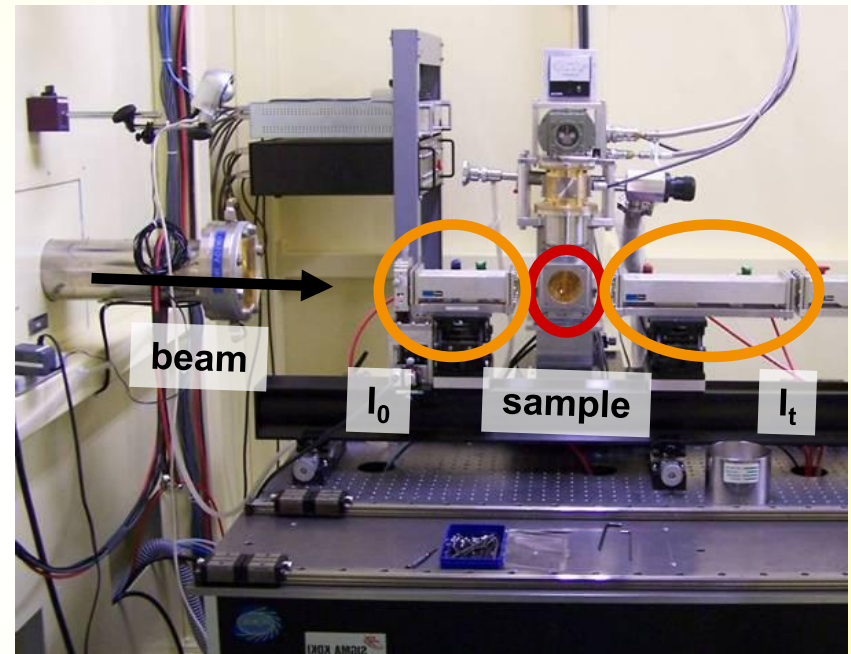
→ simple setup
high quality data

→ but samples must be:

concentrated
thick (10...50 μm)
uniform



→ **typically powder samples**

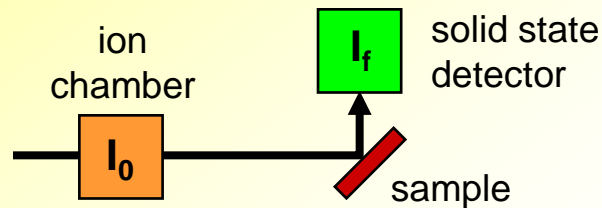


NW10-A, Photon Factory, Japan

Experimental techniques

Detection modes

Fluorescence



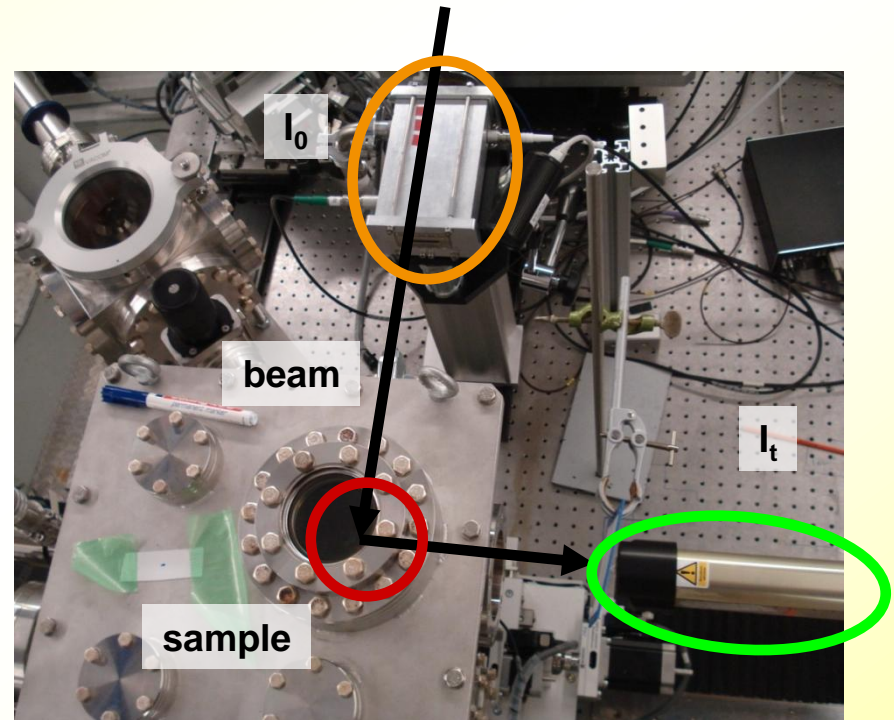
→ bulk sensitive

→ sophisticated detector
limited count rate

→ but samples can be:

diluted
thin ($\leq 2 \mu\text{m}$)
nonuniform

} → **thin films, nanoparticles, ...**

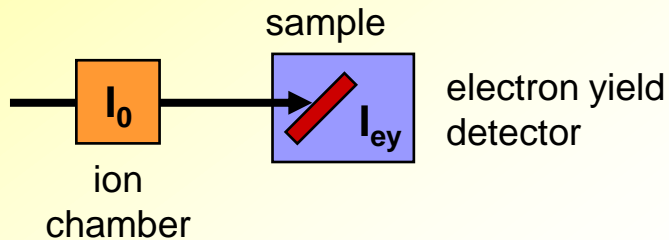


SuperXAS, SLS, Switzerland

Experimental techniques

Detection modes

Electron yield

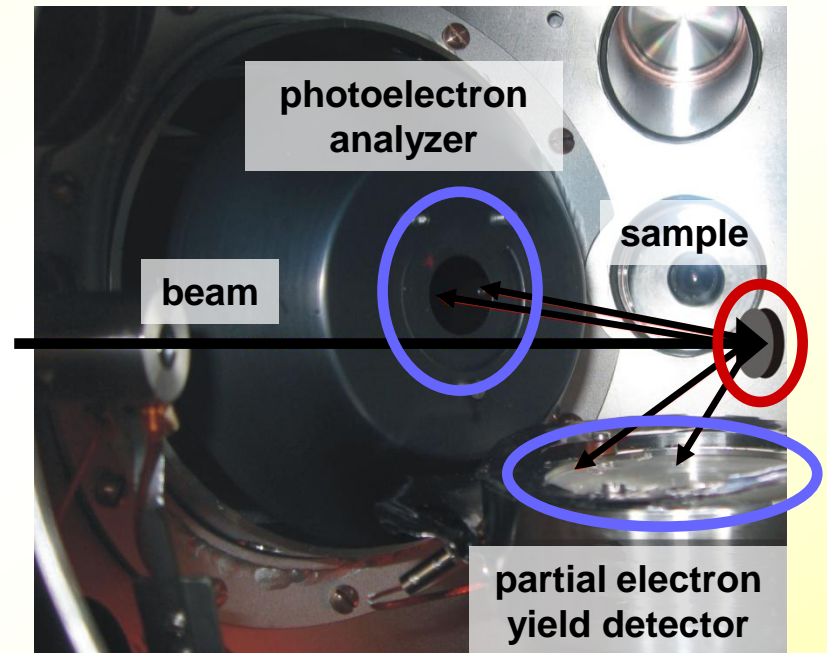


→ surface sensitive
(~ 100 nm)

→ sophisticated detector
ultra high vacuum

→ **suitable for light elements
(soft X-ray regime)**

but surface treatment of sample may be necessary



D1011, **MAX II**, Sweden

www.maxlab.lu.se/node/458

Experimental techniques

Specialized techniques - I

Grazing incidence XAS

reduced penetration depth

→ highly surface sensitive (tens of nm)

Total external reflection XAS

penetration depth further reduced

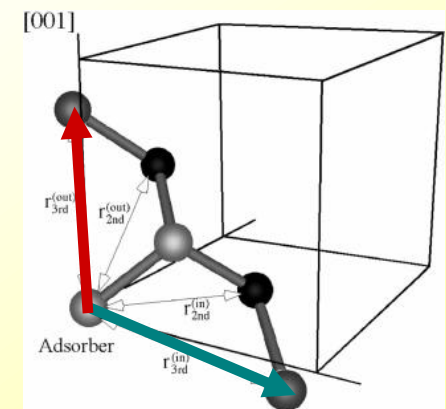
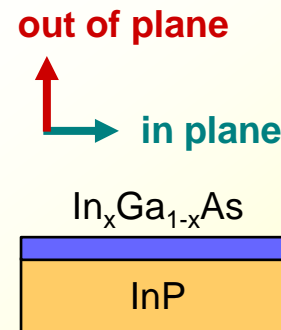
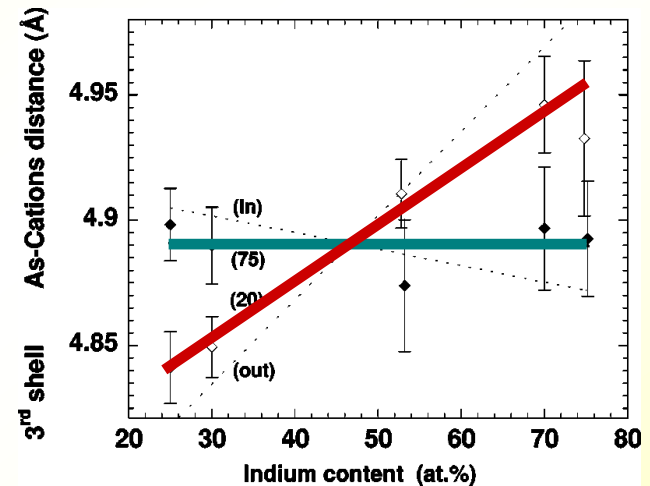
→ extremely surface sensitive (some nm)

Polarization-dependent XAS

absorption coefficient depends

on X-ray polarization

→ structural parameters parallel and perpendicular to sample normal



Tormen et al., PRB 63, 2001



Experimental techniques

Specialized techniques - II

Diffraction anomalous fine structure (DAFS)

measures intensity of a particular Bragg reflection as function of the X-ray energy

- same structural information as XAS
- can provide site or spatial selectivity
e.g. $\text{In}_x\text{Ga}_{1-x}\text{As}$ layer on GaAs substrate

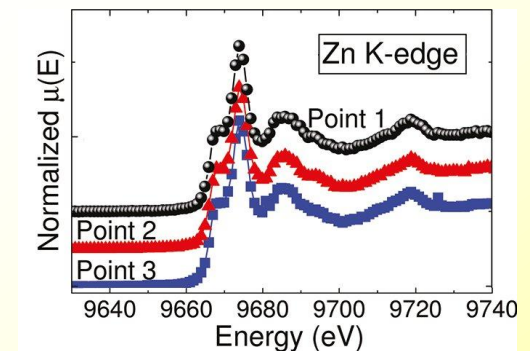
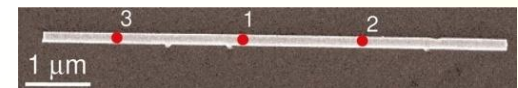
QuickXAS and energy-dispersive XAS

- time-resolved studies (s ... min)

MicroXAS

- spatially resolved studies (tens of nm ... μm)

Co-doped ZnO nanowire



*Segura-Ruiz et al.,
Nano Lett. 11, 2011*

but: all techniques require specialized setup and much experience

Contents – Part II

X-ray sources ✓

Experimental techniques ✓

Sample preparation

Data analysis

XANES

EXAFS

Summary



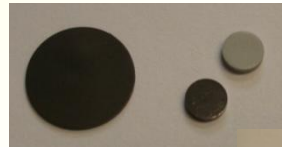
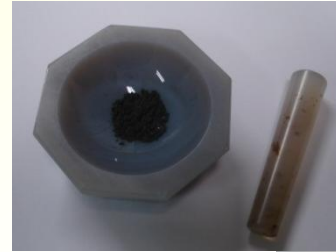
Sample preparation

powders

grinding and dilution with binder,
e.g. BN, graphite or cellulose

→ ball mill or mortar

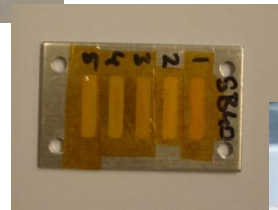
pressing into pellets
or sample holder
or dispersion on tape



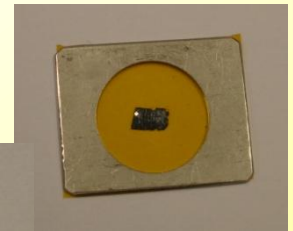
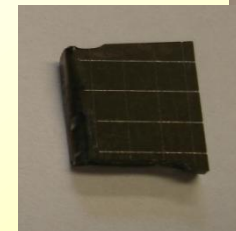
thin films

measure as-grown on substrate
or lifted off on tape

alternatively: scrape off and process
as powder sample



Matt Newville



many more options for other types of samples ...

Contents – Part II

X-ray sources ✓

Experimental techniques ✓

Sample preparation ✓

Data analysis

XANES

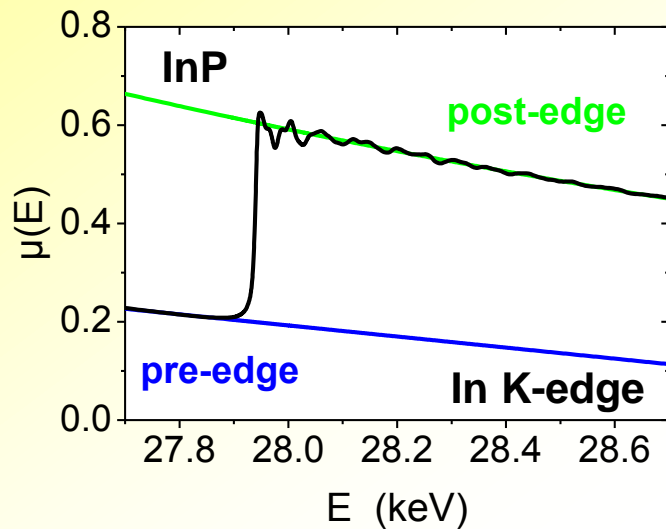
EXAFS

Summary



XANES analysis

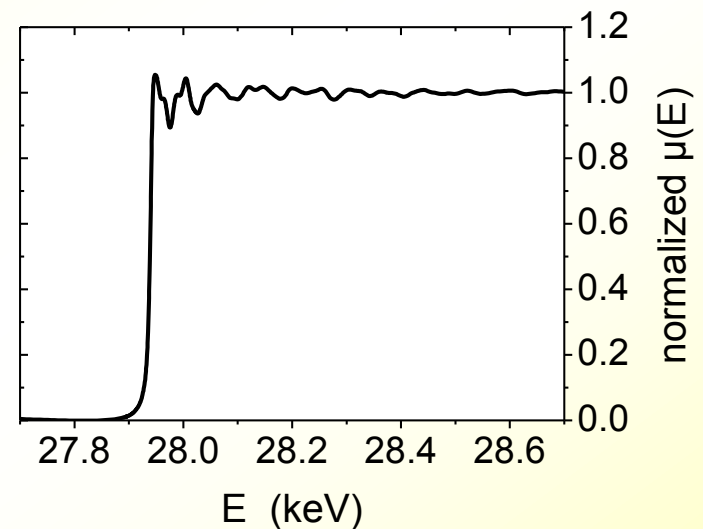
Normalization



*Schnohr et al.,
PRB 79, 2009*



IFEFFIT
software
package:
ATHENA



energy calibration
alignment of spectra
→ reference samples

Newville & Ravel
<http://cars9.uchicago.edu/ifeffit>

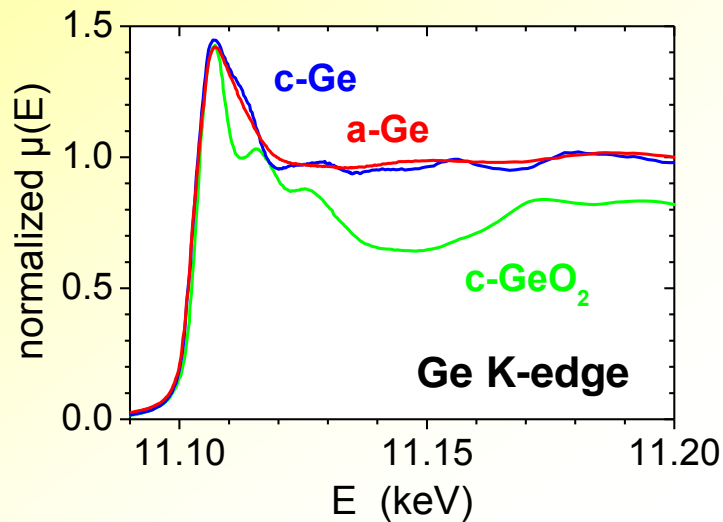
normalization of spectra
→ uses pre-edge and
post-edge lines

→ possible to compare spectra of different samples



XANES analysis

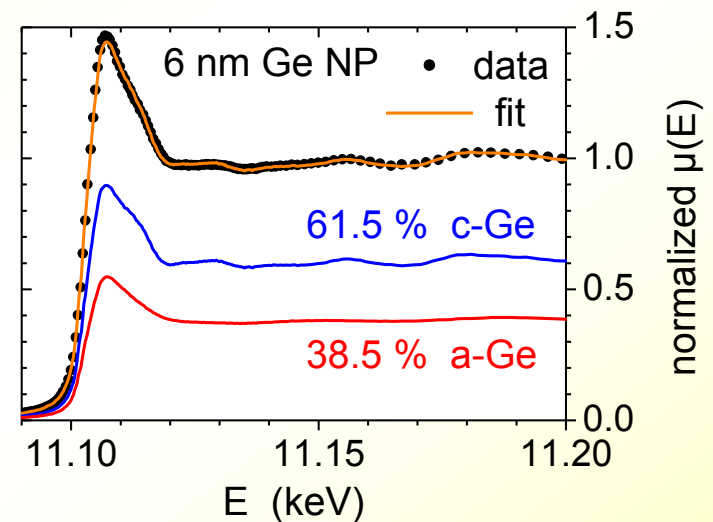
Linear combination fitting



Araujo et al.,
PRB78, 2008



ATHENA



comparison of measured spectra to those of known standards

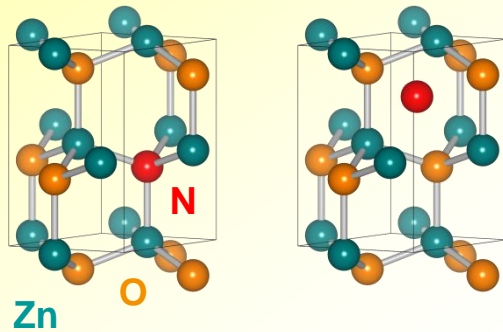
→ linear combination fitting

but: existence and measurement of suitable standards is crucial

XANES analysis

Theoretical calculations

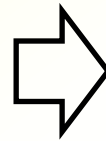
different structural models



N in ZnO

e.g. from density functional theory (DFT)

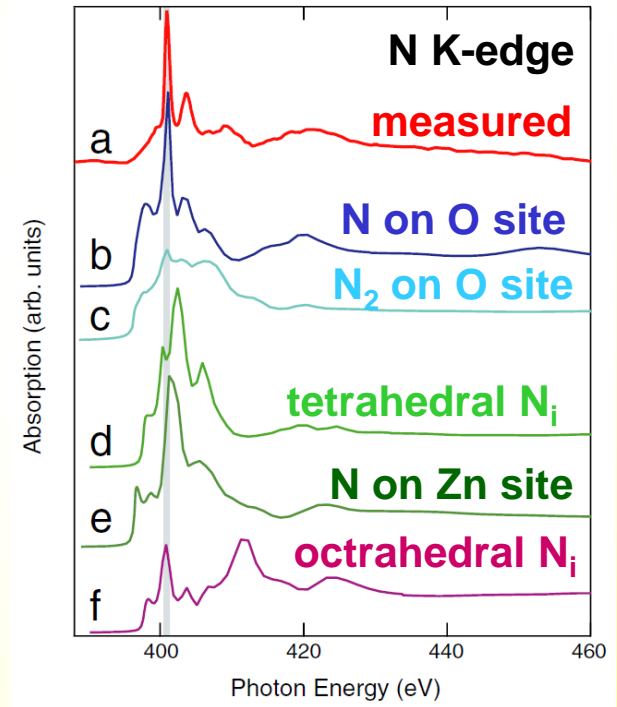
calculation of theoretical spectra



computer code FEFF

Rehr et al.

<http://www.fefferproject.org/>



Fons et al., PRL 96, 2006

comparison of calculated with measured spectra

→ acceptance or rejection of structural models

but: complicated and accuracy is sometimes limited



Contents – Part II

X-ray sources ✓

Experimental techniques ✓

Sample preparation ✓

Data analysis

XANES

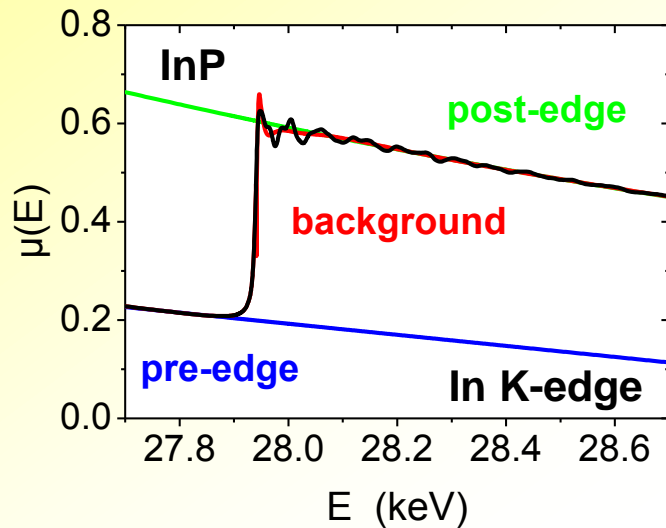
EXAFS

Summary



EXAFS analysis

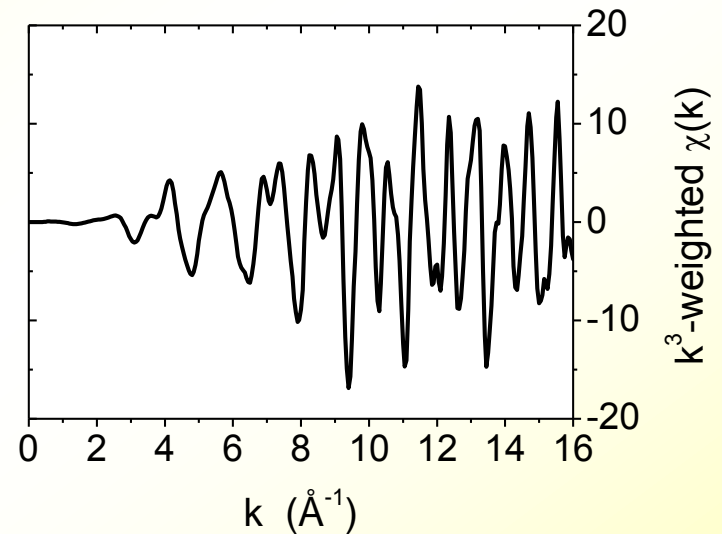
Data processing



*Schnohr et al.,
PRB 79, 2009*



ATHENA



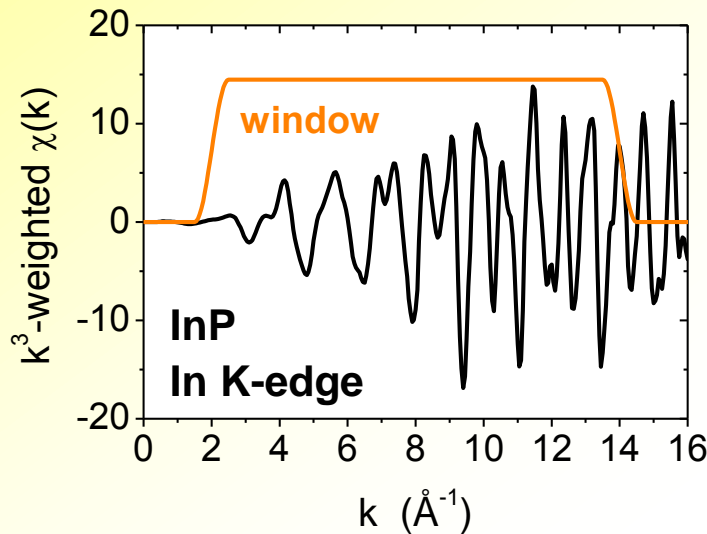
background subtraction
→ isolated fine structure

energy scale is converted
to photoelectron wave number

$$k = \sqrt{2m_e(E - E_B)/\hbar}$$

EXAFS analysis

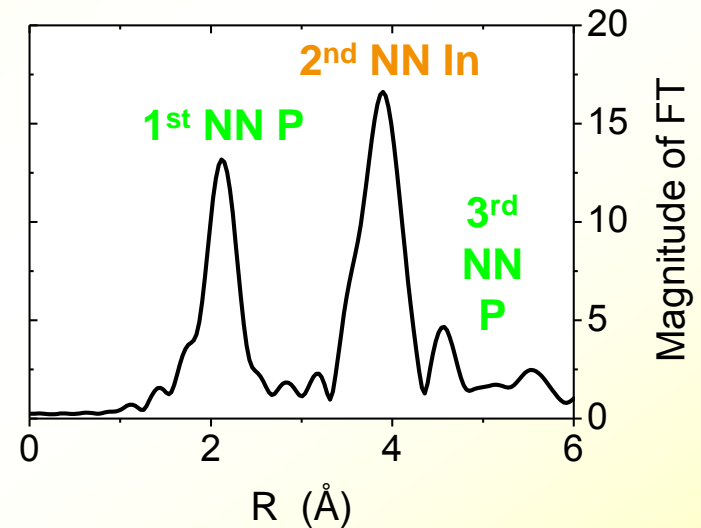
Data processing



Schnohr et al.,
PRB 79, 2009



ATHENA



background subtraction
→ isolated fine structure

Fourier transformation (FT)
→ visualization of different scattering contributions

→ analysis of different scattering contributions



EXAFS analysis

Ratio Method

analysis of difference between
unknown sample and known reference

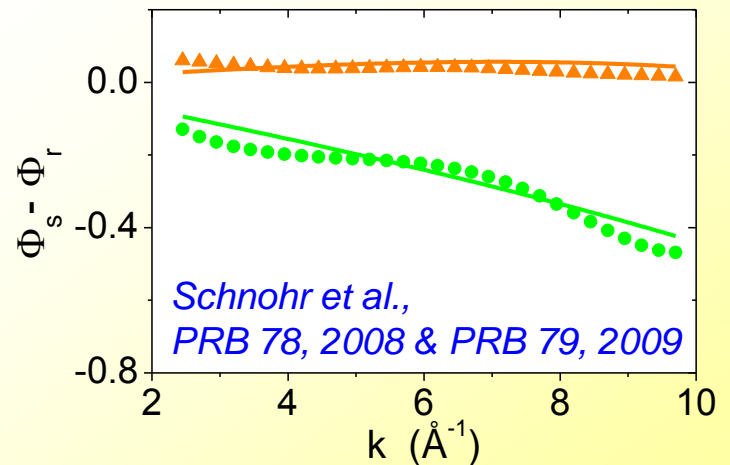
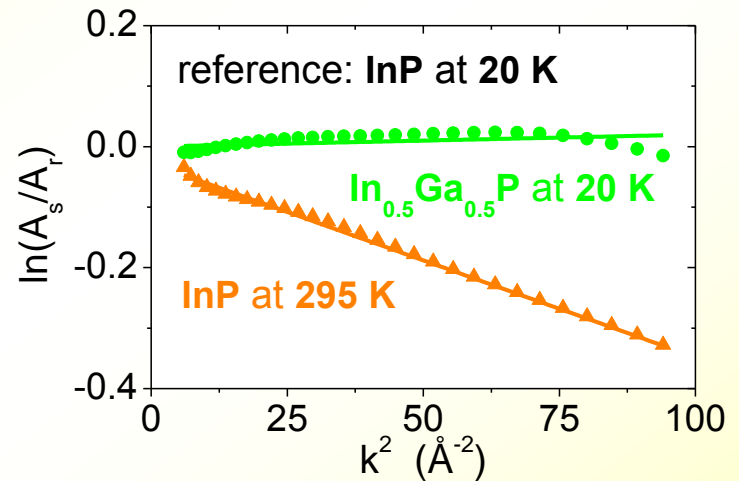
amplitude:

$$\ln \left| \frac{A_s(k)}{A_r(k)} \right| = C - 2k^2(\sigma_s^2 - \sigma_r^2) + \dots$$

phase:

$$\Phi_s(k) - \Phi_r(k) = 2k(R'_s - R'_r) - \dots$$

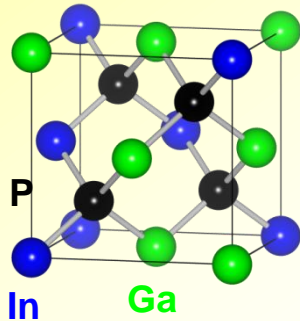
→ **no structural model needed**
but: limited to first shell
requires suitable reference



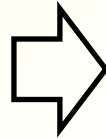
EXAFS analysis

Path fitting

structural model



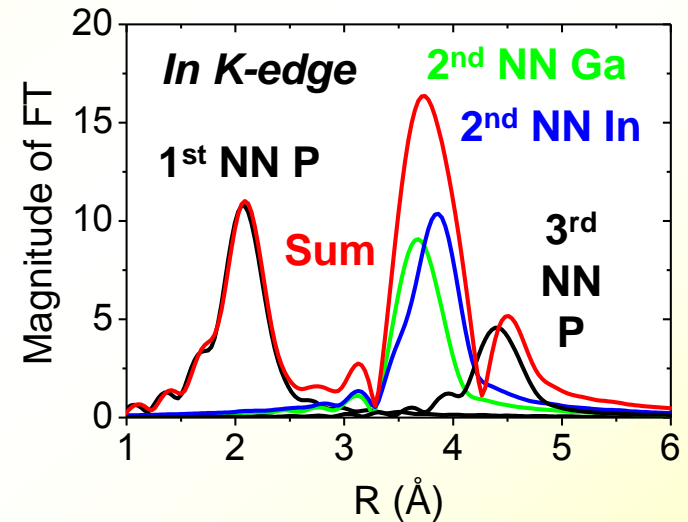
calculation of
theoretical spectrum



computer code FEFF

Rehr et al.

<http://www.fefferproject.org/>



refinement of structural parameters by fitting calculated to measured spectra

- **analysis of mixed and higher shells**
- no reference material needed**
- but: requires structural model**

IFEFFIT software
package: ARTEMIS

Newville & Ravel

<http://cars9.uchicago.edu/ifeffit>



Contents – Part II

X-ray sources ✓

Experimental techniques ✓

Sample preparation ✓

Data analysis ✓

XANES

EXAFS

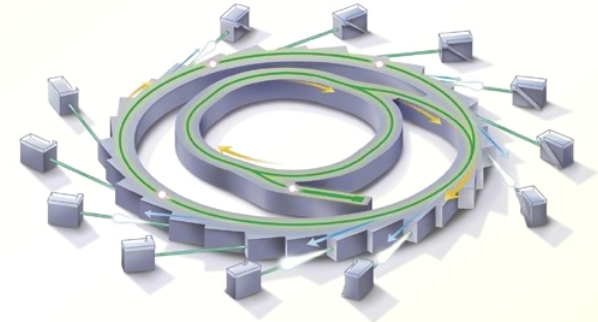
Summary



Summary

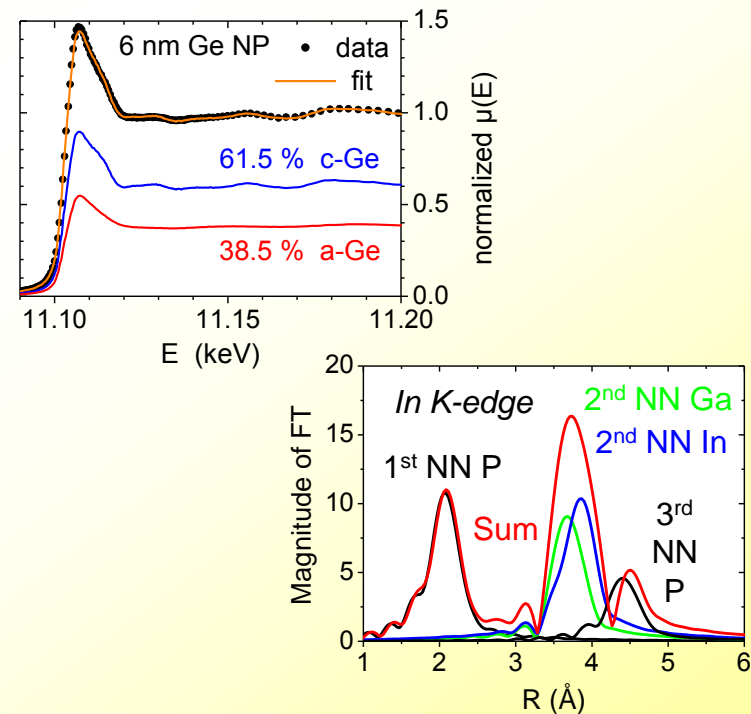
XAS measurements

- synchrotron radiation
- transmission, fluorescence or electron yield mode
- specialized techniques
- powders, thin films, ...



analysis

- XANES → data normalization
→ linear combination fitting
→ theoretical calculations
- EXAFS → data processing
→ Ratio Method
→ path fitting



Part I Basics of XAS

Part II Experimental aspects of XAS

Part III Applications of XAS to chalcopyrite and kesterite materials

Contents – Part III

Chalcopyrites

Atomic-scale structure and band gap bowing

Local versus global electronic properties

Cu content and Cu-poor phases

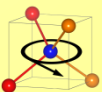
Kesterites

Secondary phases

Cation disorder

Atomic-scale structure

Conclusions

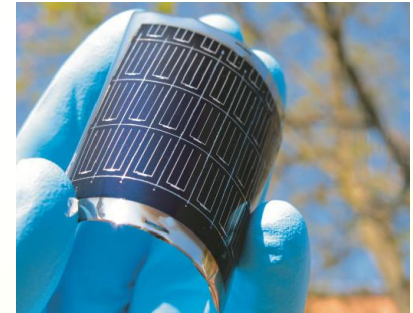


Cu(In,Ga)Se₂

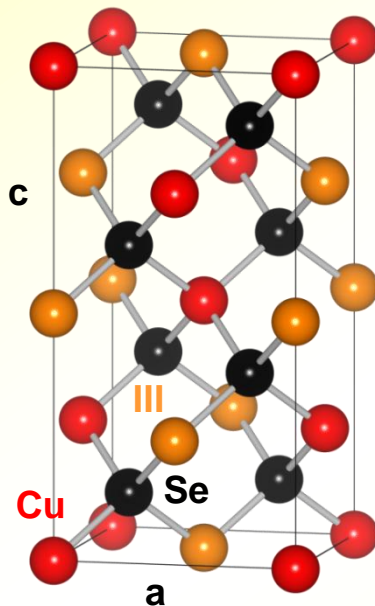
Crystal structure

thin film solar cells with record efficiencies above 20 %
on glass and polymer foils

Jackson et al., PPRA 19, 2011
Chirila et al., Nature Mat. 12, 2013



Chalcopyrite structure



space group $I\bar{4}2d$

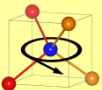
a and c change linearly with In/III (Vegard's Law)

anion (Se) displacement

CuGaSe₂ $d_{\text{Cu-Se}} \sim d_{\text{Ga-Se}}$ \rightarrow Se not displaced

CuInSe₂ $d_{\text{Cu-Se}} < d_{\text{In-Se}}$ \rightarrow Se displaced

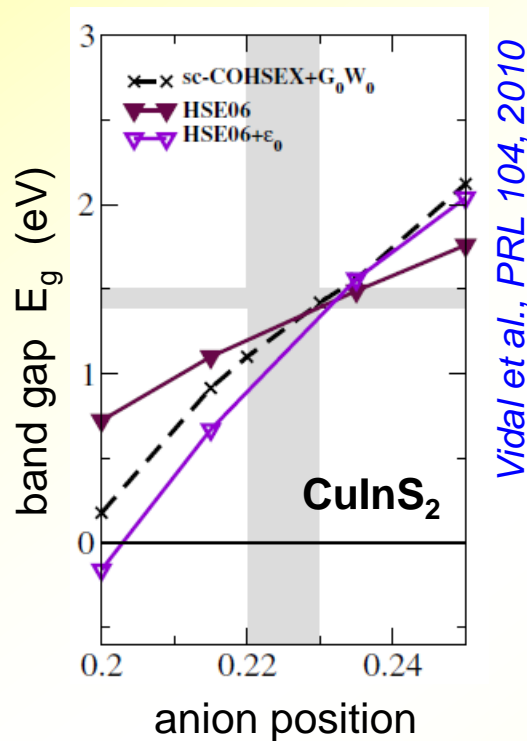
Cu(In,Ga)Se₂ \rightarrow Se position ?



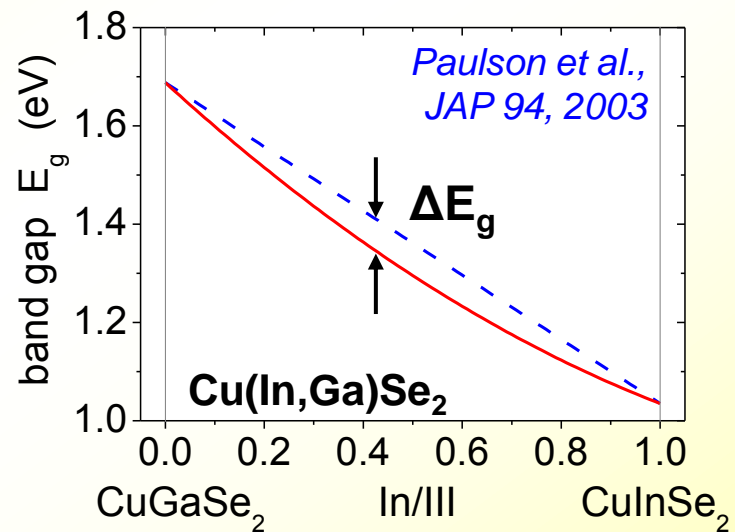
Cu(In,Ga)Se₂

Anion displacement and band gap

anion position strongly influences band gap



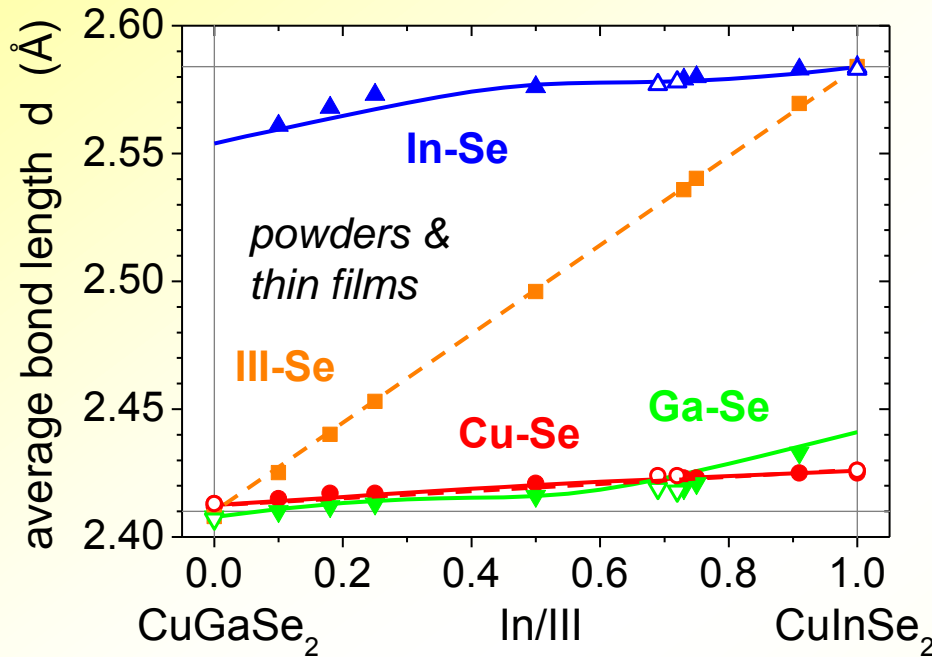
band gap changes nonlinearly with In/III
→ band gap bowing ΔE_g



→ study atomic-scale structure and influence on band gap in Cu(In,Ga)Se₂

Cu(In,Ga)Se₂

Element-specific bond lengths



→ distinctly different and nearly constant

→ average III-Se distance matches diffraction results

Schnohr et al., PRB 85, 2012

→ same bond lengths for powders and thin films

Schnohr et al., TSF, 2014

→ short-range atomic arrangements deviate significantly from long-range crystallographic structure

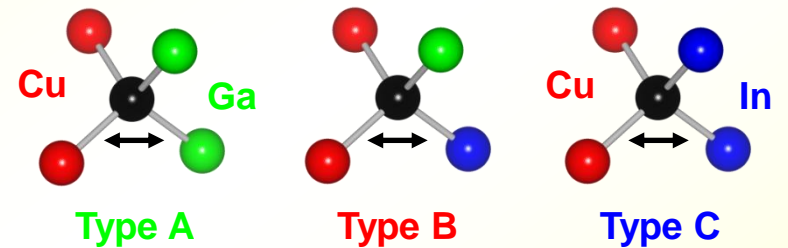
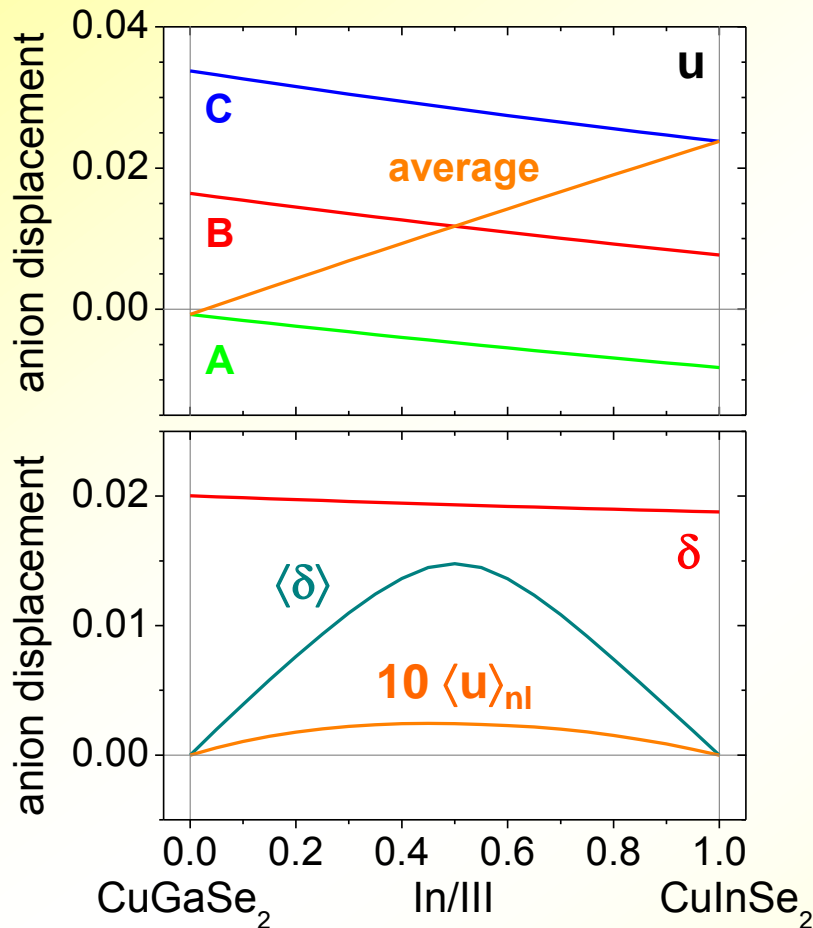
typical for tetrahedrally coordinated semiconductors

Schnohr et al., PRB 78, 2008

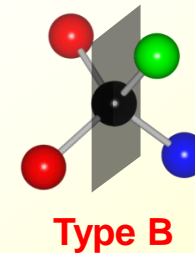


Cu(In,Ga)Se₂

Anion displacement



displacement u between Cu and III



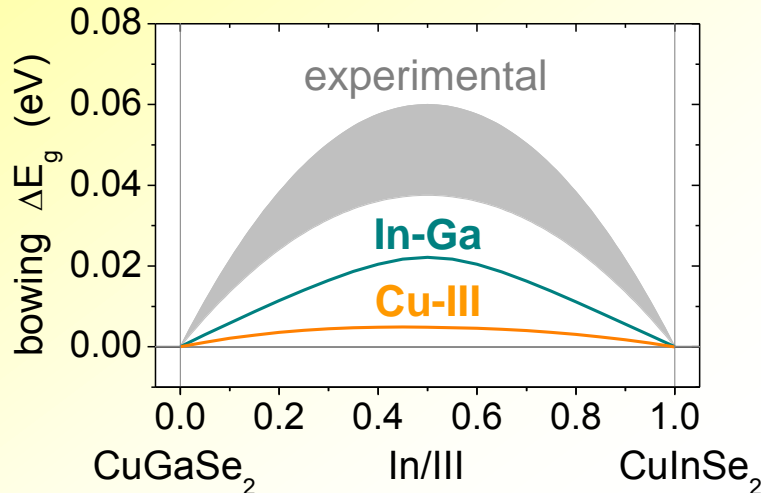
displacement δ between In and Ga

→ **two different relaxation effects**
both are nonlinear with In/III

Cu(In,Ga)Se₂

Band gap bowing

Wei & Zunger,
JAP 78, 1995



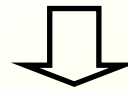
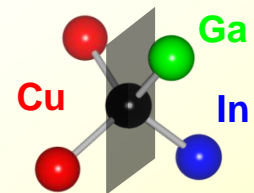
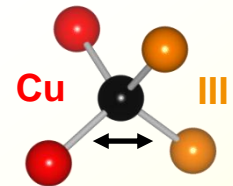
Schnohr et al.,
PRB 85, 2012

$$\Delta E_g^{Cu-III} = 20eV \cdot \langle u \rangle_{nl}$$

Vidal et al., PRL 104, 2010

$$\Delta E_g^{In-Ga} = 1.5eV \cdot \langle \delta \rangle$$

Schnohr, JPCM 24, 2012



three sources

- volume deformation
- charge redistribution
- **anion relaxation**

Bernard & Zunger., PRB 36, 1987

atomic-scale structure strongly influences material properties

→ **similar results for Cu(In,Ga)S₂**

Eckner et al., APL 103, 2013

Contents – Part III

Chalcopyrites

Atomic-scale structure and band gap bowing ✓

Local versus global electronic properties

Cu content and Cu-poor phases

Kesterites

Secondary phases

Cation disorder

Atomic-scale structure

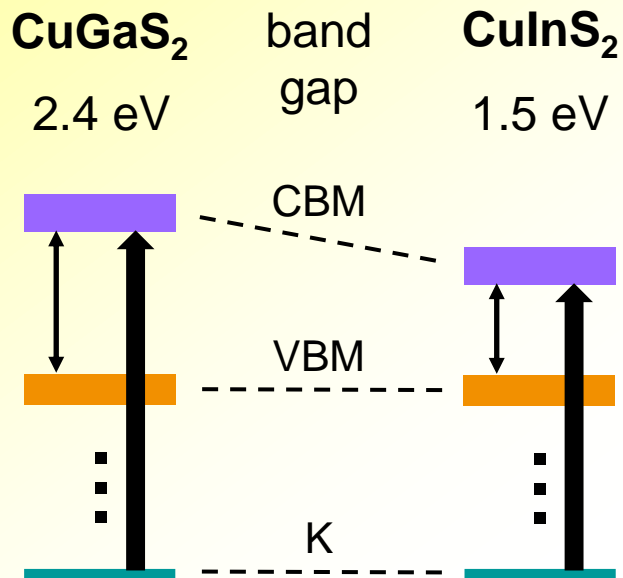
Conclusions



Cu(In,Ga)S₂

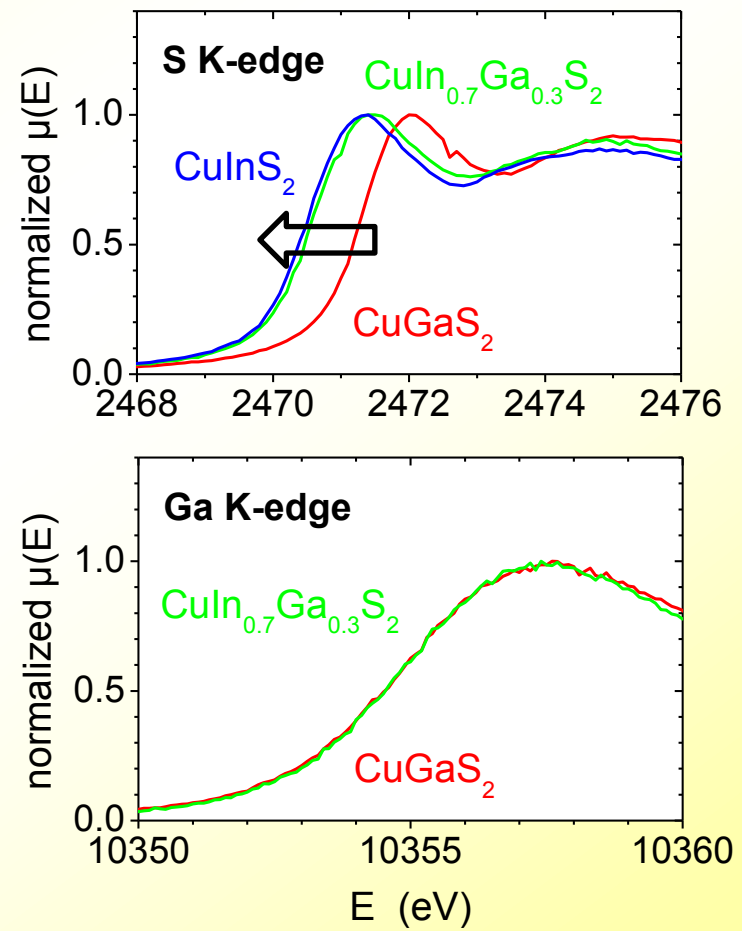
XANES

Johnson et al.
JES 190, 2013



→ absorption edge should shift with changing In/III

⇒ **S** → edge shifts
Ga, In, Cu → no shift



Cu(In,Ga)S₂

Density of states

ab initio DFT-based calculations

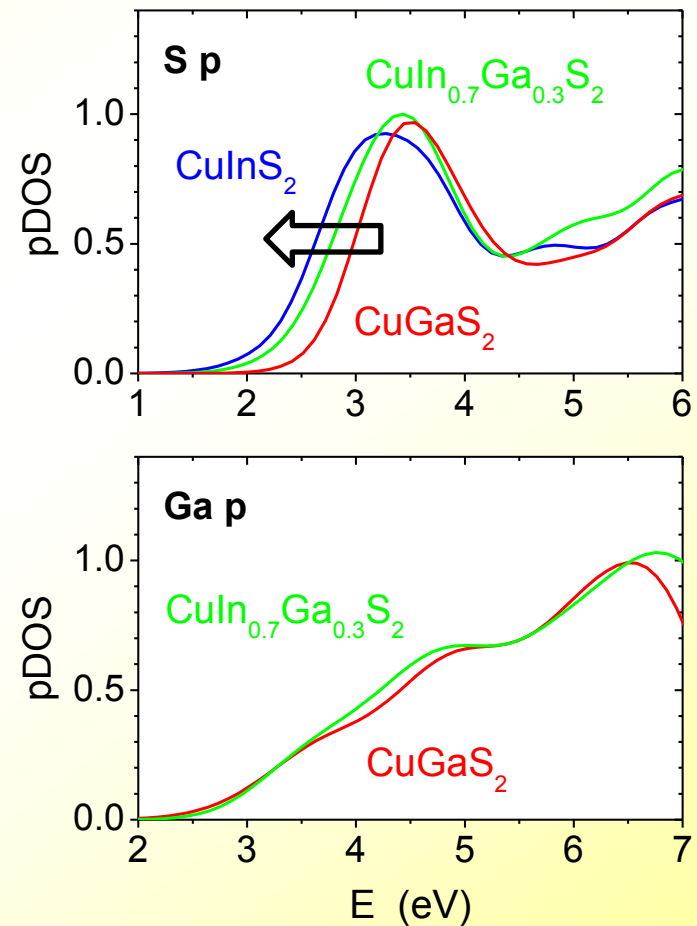
using hybrid functionals and
special quasi-random structures

Sarmiento-Pérez et al., JAP 116, 2014

→ projected partial density
of states (pDOS)
corresponding to unoccupied
states probed by XANES

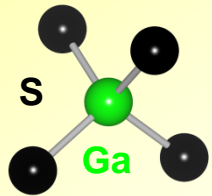
⇒ **S → edge shifts**
Ga, In, Cu → no shift

despite change in band gap
cation edges don't shift → Why ?

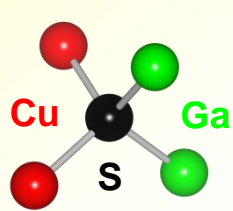
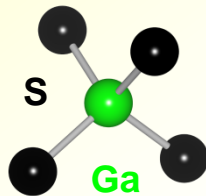
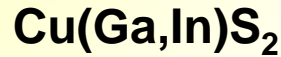


Cu(In,Ga)S₂

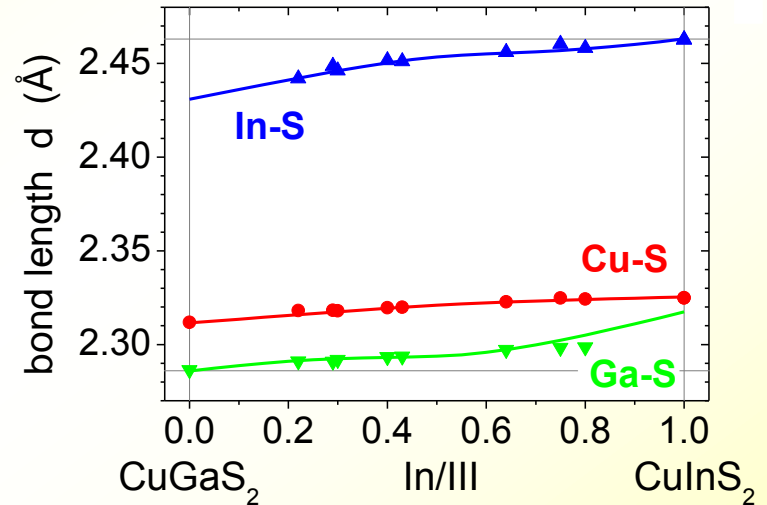
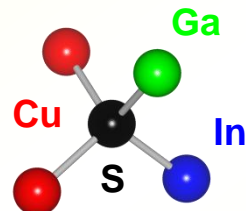
Local atomic environment



→ no change for Ga, In and Cu



→ local environment around S changes



Eckner et al., APL 103, 2013

Sarmiento-Pérez et al., JAP 116, 2014

→ **local environment determines local electronic states**
change in band gap due to changing spatial average

Contents – Part III

Chalcopyrites

Atomic-scale structure and band gap bowing ✓

Local versus global electronic properties ✓

Cu content and Cu-poor phases

Kesterites

Secondary phases

Cation disorder

Atomic-scale structure

Conclusions



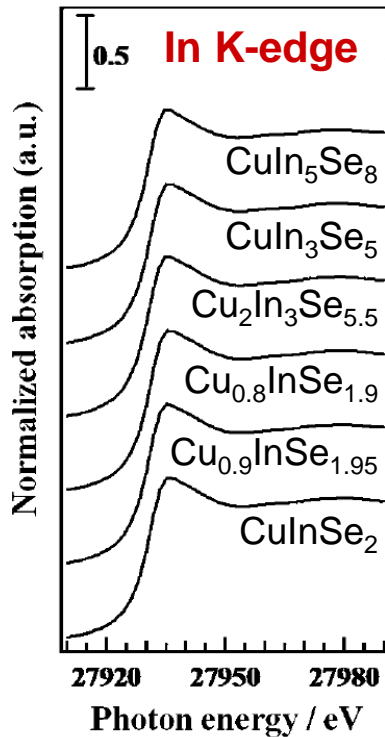
CuInSe₂ ... CuIn₅Se₈

XANES

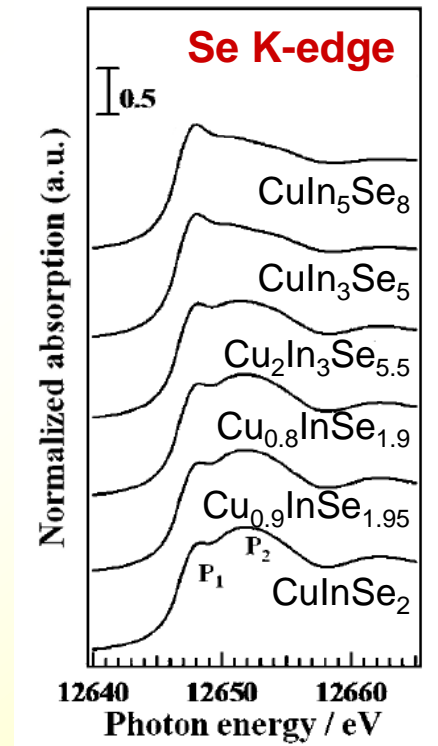
Cu poor phases

different crystal structures
but still tetrahedral coordination

- each In or Cu has four Se neighbours
bond lengths are similar for all compounds
- each Se has Cu, In and vacancy neighbours
ratio strongly changes for different compounds



→ **no change**

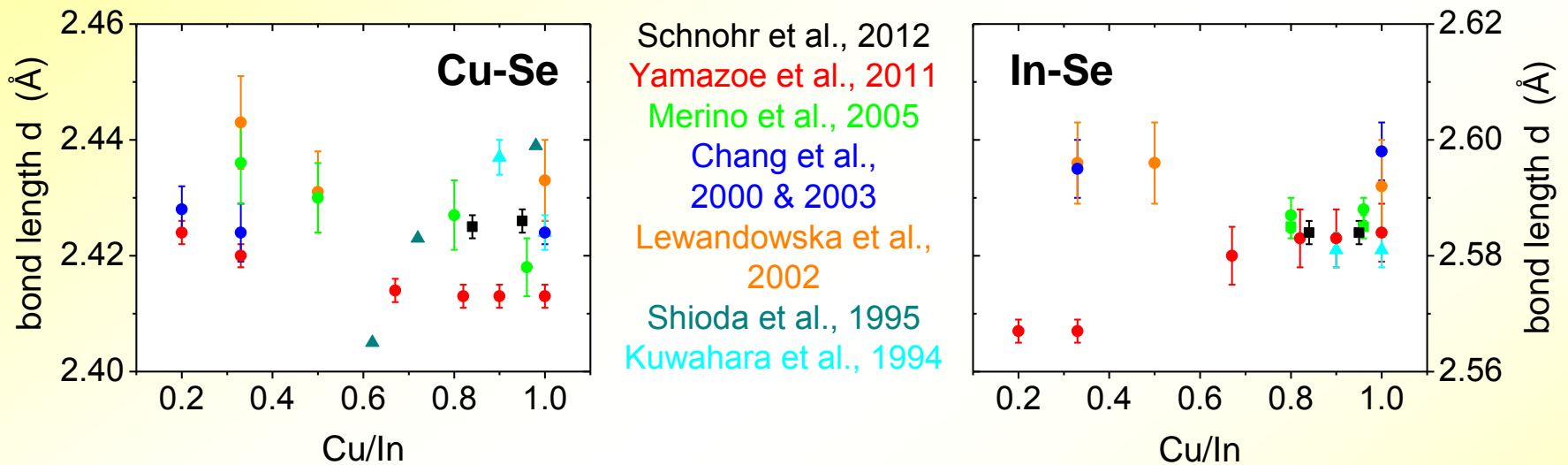


→ **strong change**

Yamazoe et al., JMR 26, 2011

CuInSe₂ ... CuIn₅Se₈

Element-specific bond lengths



→ mostly constant for $0.8 \leq \text{Cu/In} \leq 1.0$, i.e. chalcopyrite range

→ small increase or decrease for $\text{Cu/In} \leq 0.8$

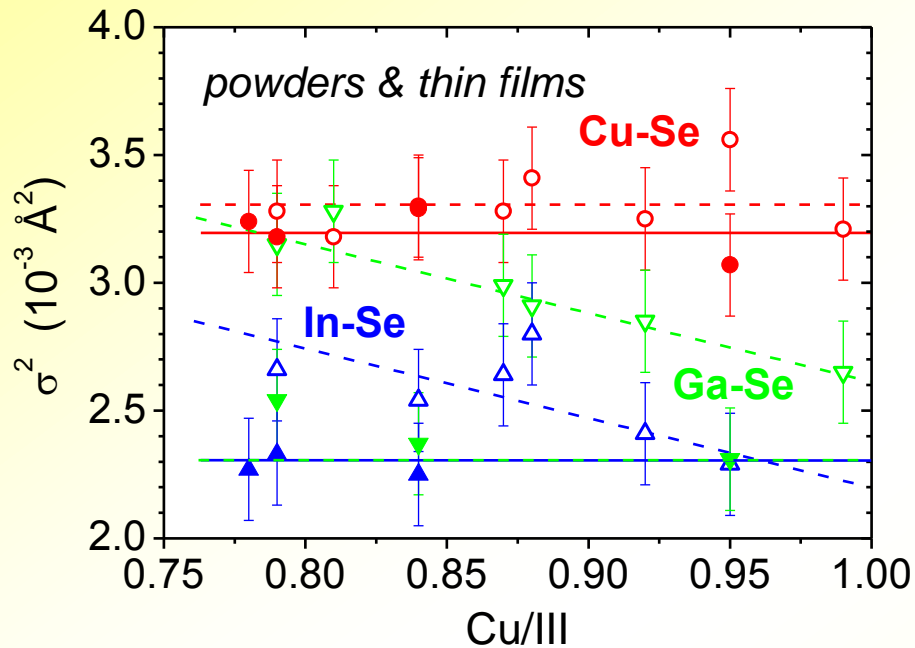
but: partly contradicting results and only Cu-In-Se system

→ **detailed study of Cu(In,Ga)₃Se₅ and Cu(In,Ga)₅Se₈**



Cu(In,Ga)Se₂

Bond length variation



Schnohr et al., TSF, 2014

powders

- Cu-Se ≥ Ga-Se ≥ In-Se
bond stretching force constants
- increase with decreasing Cu/III
increasing amount of defects

thin films

- Ga-Se and In-Se smaller than
powders especially for low Cu/III
different Cu history, i.e. Cu-rich
state during co-evaporation

→ bond length variation depends on cation-anion pair
and probably on Cu/III history during preparation

Contents – Part III

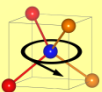
Chalcopyrites

- Atomic-scale structure and band gap bowing ✓
- Local versus global electronic properties ✓
- Cu content and Cu-poor phases ✓

Kesterites

- Secondary phases
- Cation disorder
- Atomic-scale structure

Conclusions



$\text{Cu}_2\text{ZnSnS}_4$

Crystal structure

thin film solar cells made of earth-abundant and non-toxic elements

record efficiency for $\text{Cu}_2\text{ZnSn}(\text{S},\text{Se})_4$ 12.6 %

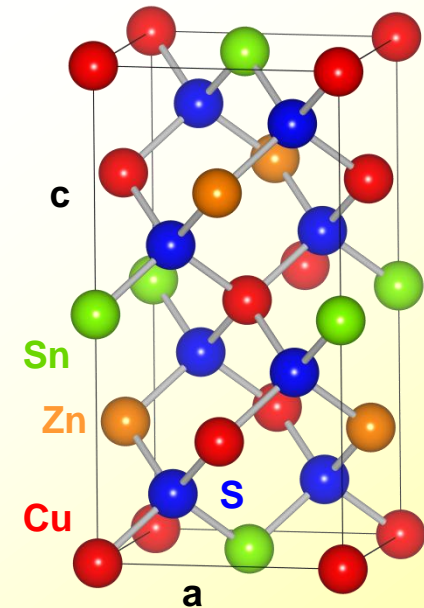
Wang et al., AEM 4, 2014

but: preparation often yields admixture of

- (a) secondary phases with different composition
e.g. ZnS, CuS, SnS_2 , ...
- (b) secondary phases with different crystal structure
that features different cation ordering
e.g. Stannite (space group $I\bar{4}2m$), ...

Kesterite structure

space group $I\bar{4}$



secondary phases affect electronic properties → have to be avoided

Cu₂ZnSnS₄

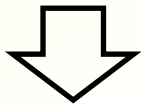
XANES

admixture of ZnS to Cu₂ZnSnS₄ very difficult to detect with diffraction

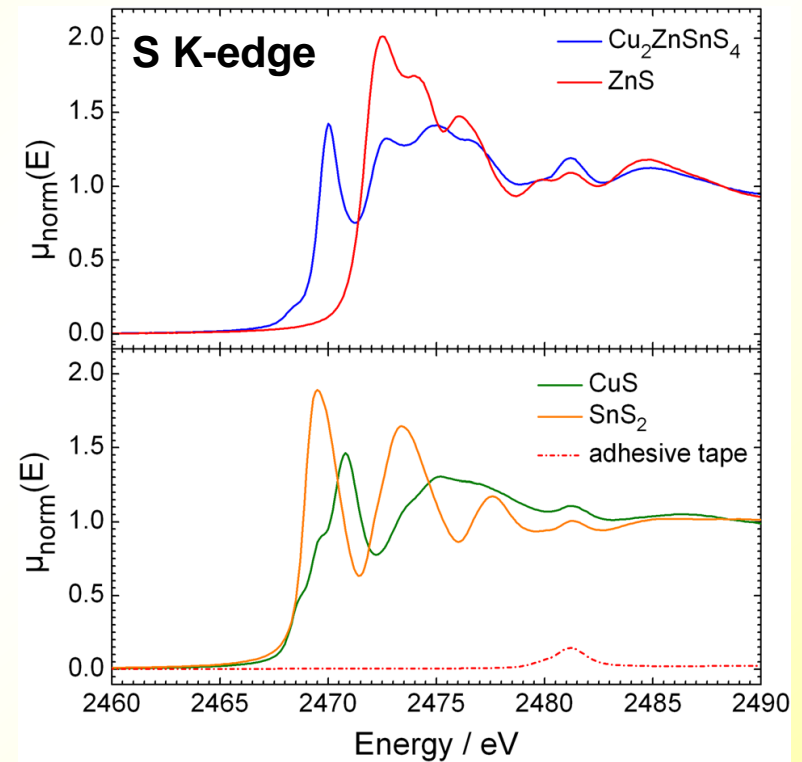
→ different method needed

S K-edge XANES spectra

→ distinctly different for Cu₂ZnSnS₄ and ZnS, CuS, SnS₂



quantitative determination of secondary phases, e.g. ZnS, by linear combination fitting

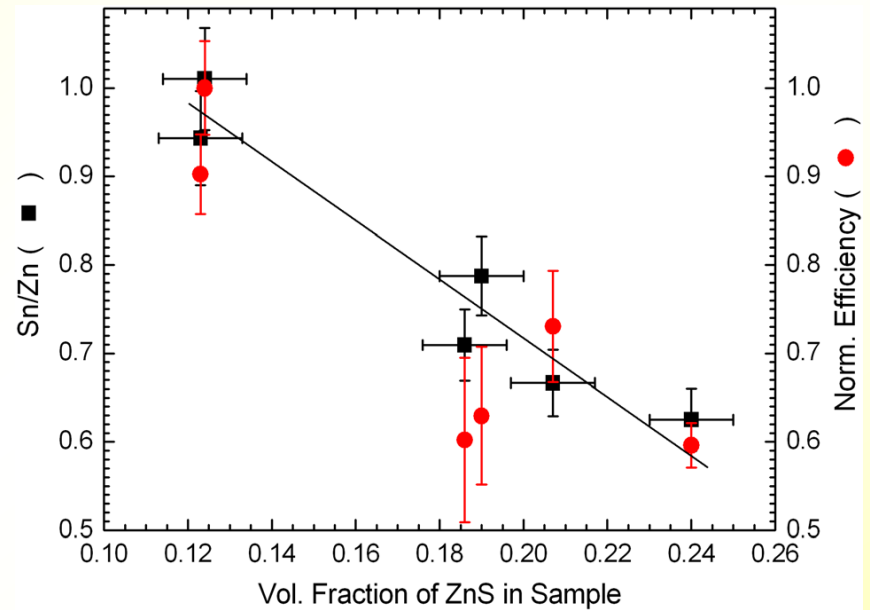
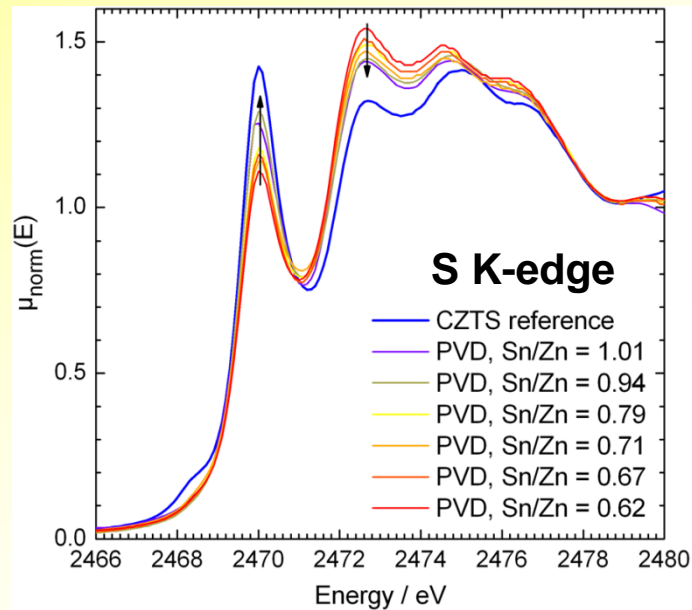


Just et al., APL 99, 2011



Cu₂ZnSnS₄

Amount of ZnS secondary phase



Just et al., APL 99, 2011

→ amount of ZnS increases for decreasing Sn/Zn ratio

→ efficiency decreases for increasing amount of ZnS



Contents – Part III

Chalcopyrites

- Atomic-scale structure and band gap bowing ✓
- Local versus global electronic properties ✓
- Cu content and Cu-poor phases ✓

Kesterites

- Secondary phases ✓
- Cation disorder
- Atomic-scale structure

Conclusions

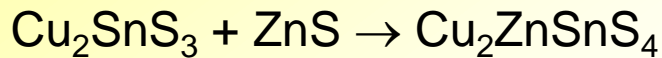


Cu₂ZnSnS₄

Cation disorder

nanoparticle synthesis

Zillner et al., APL 102, 2013

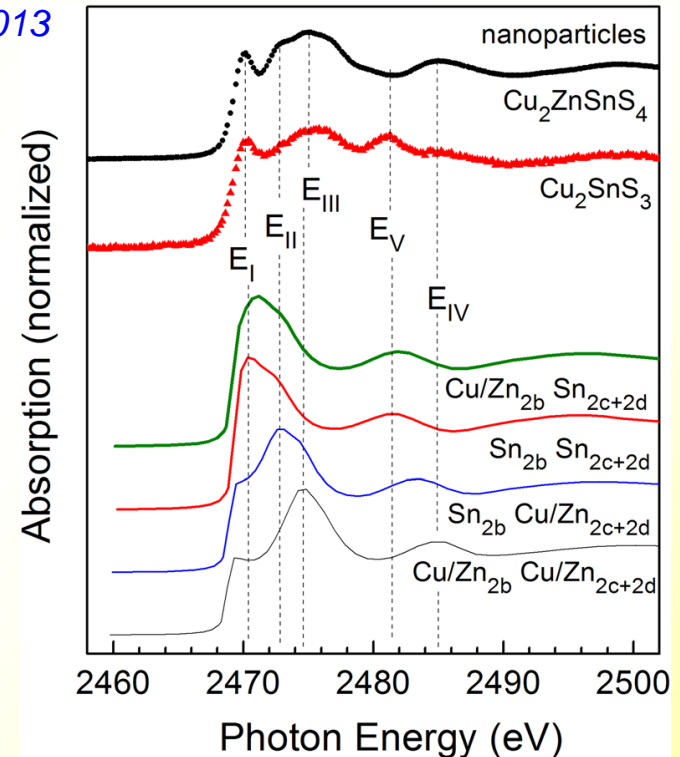
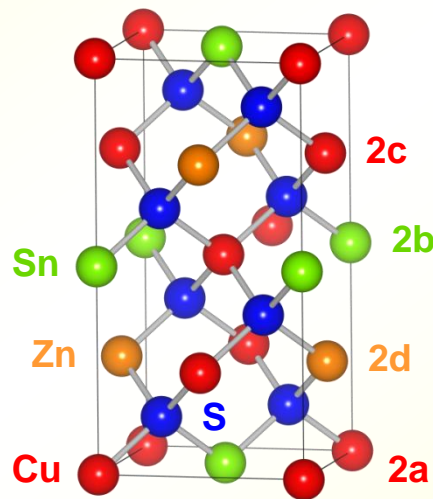


→ cation distribution ?

calculation of S K-edge XANES for different cation distributions

→ cannot distinguish Cu and Zn

→ but is sensitive to Sn-Cu/Zn antisites and Sn vacancies



→ cation distribution depending on synthesis and/or treatment

Contents – Part III

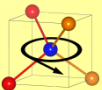
Chalcopyrites

- Atomic-scale structure and band gap bowing ✓
- Local versus global electronic properties ✓
- Cu content and Cu-poor phases ✓

Kesterites

- Secondary phases ✓
- Cation disorder ✓
- Atomic-scale structure

Conclusions

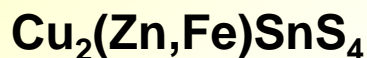


$\text{Cu}_2(\text{Zn,Fe})\text{SnS}_4$

Element-specific bond length

kesterite
 $\text{Cu}_2\text{ZnSnS}_4$

stannite
 $\text{Cu}_2\text{FeSnS}_4$

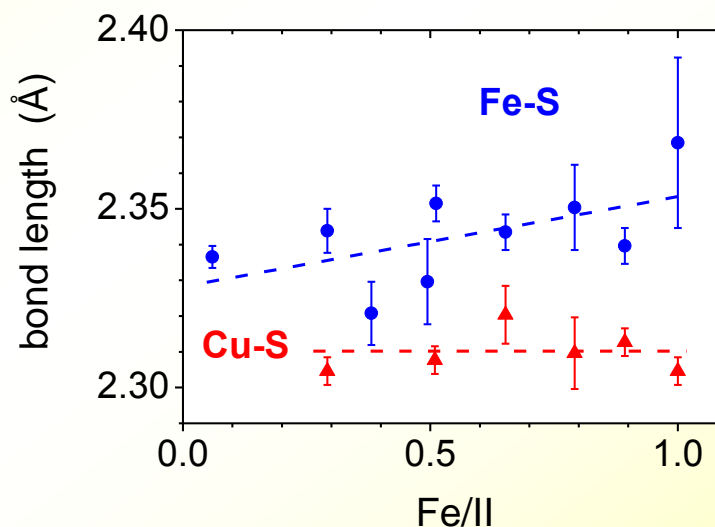


Cu-S and Fe-S bond lengths

→ different from each other

→ different slope with Fe/II

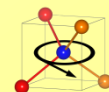
→ **different behaviour than chalcopyrites**



Zalewski et al., JAC 492, 2010

→ **detailed study of mixed kesterites**

influence of atomic-scale structure on band gap



Contents – Part III

Chalcopyrites

- Atomic-scale structure and band gap bowing ✓
- Local versus global electronic properties ✓
- Cu content and Cu-poor phases ✓

Kesterites

- Secondary phases ✓
- Cation disorder ✓
- Atomic-scale structure ✓

Conclusions

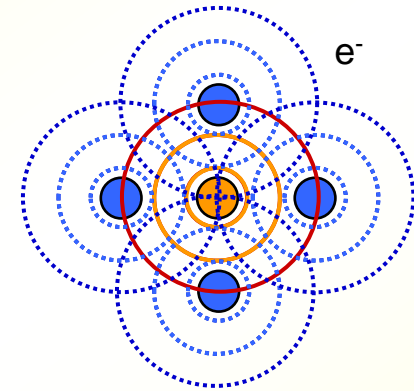


Conclusions

Basics of XAS

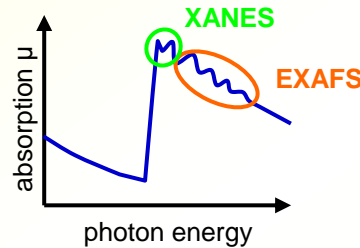
X-ray absorption spectroscopy (XAS)

- structural analysis on sub-nm scale
- crystalline and disordered solids, liquids, ...
- element-specific



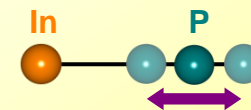
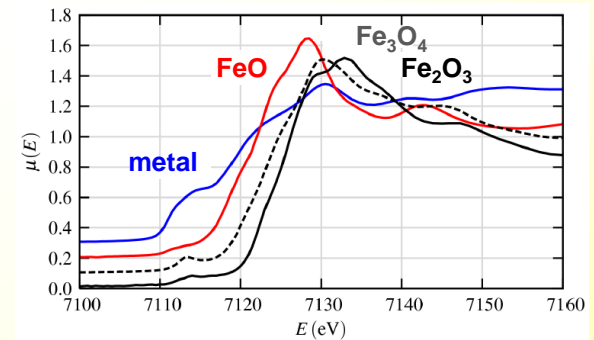
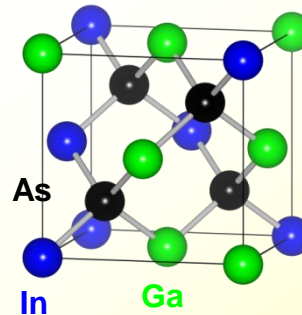
XANES

- density of states, chemical bonding
- crystal or cluster symmetry



EXAFS

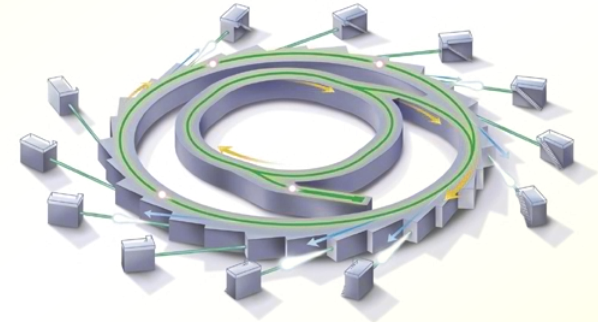
- coordination number
- bond lengths
- static disorder
- atomic vibrations



Experimental aspects

XAS measurements

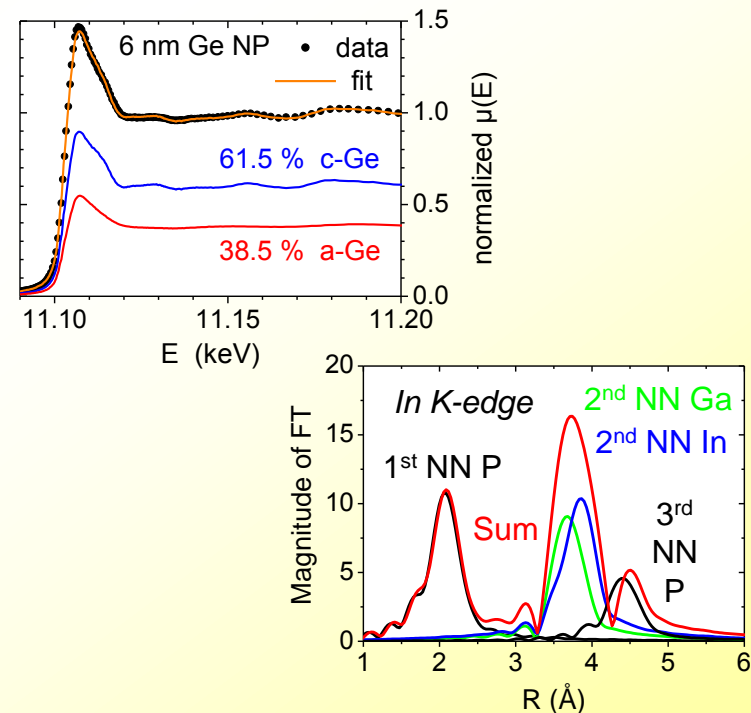
- synchrotron radiation
- transmission, fluorescence or electron yield mode
- specialized techniques
- powders, thin films, ...



analysis

- XANES → data normalization
→ linear combination fitting
→ theoretical calculations

- EXAFS → data processing
→ Ratio Method
→ path fitting



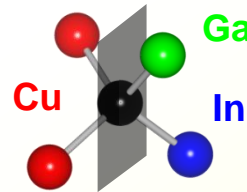
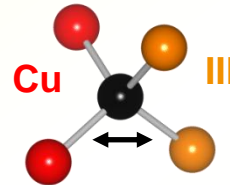
Chalcopyrites

element-specific bond lengths

- very different and nearly constant
- local arrangements deviate from crystallographic structure

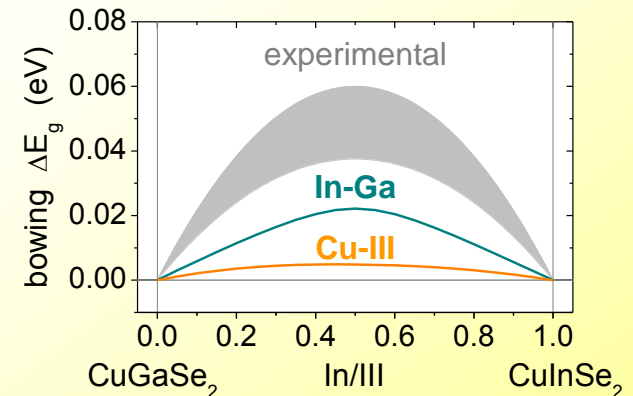
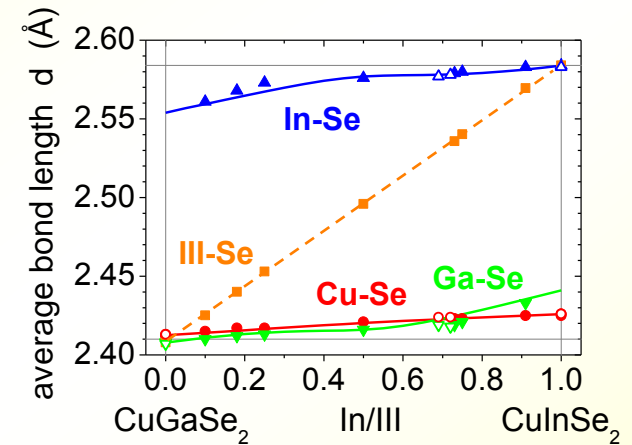
anion displacement

- depends on cation configuration
- two different displacement mechanisms



band gap bowing

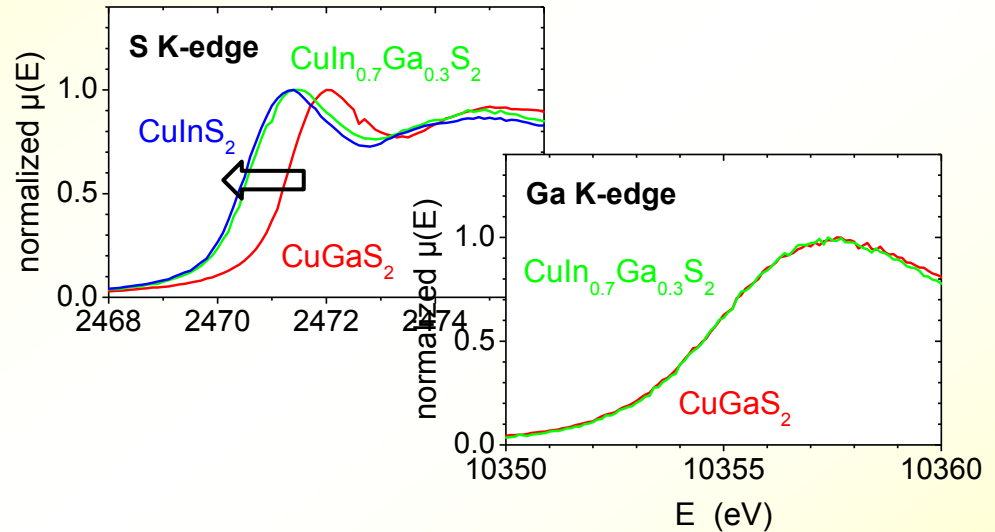
- both displacement mechanisms contribute to band gap bowing but in different ways



Chalcopyrites

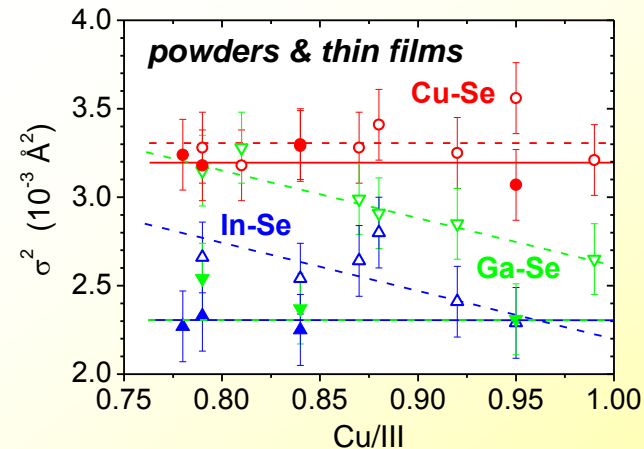
electronic states

- local states determined by local environment
- global properties like band gap arise from spatial average



bond length variation

- depends on cation-anion pair
- different for powders and thin films
- probably depends on Cu/III history during preparation



Kesterites

secondary phases

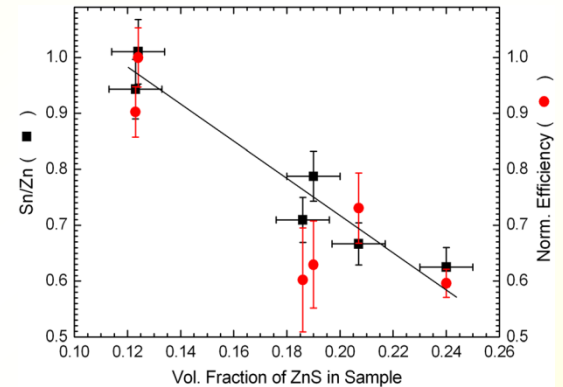
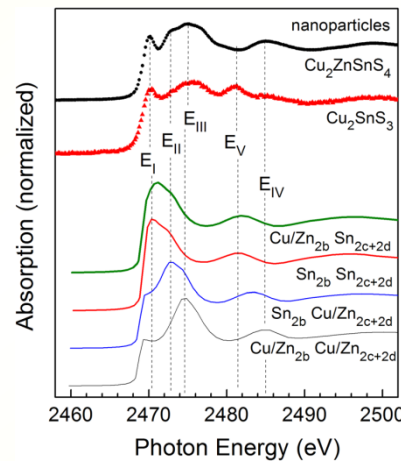
- S K-edge XANES very different for $\text{Cu}_2\text{ZnSnS}_4$ and ZnS , CuS , SnS_2 , ...
- quantitative determination of secondary phase, e.g. ZnS

cation disorder

- S K-edge XANES depends on cation distribution
- Sn-Cu/Zn antisites and Sn vacancies

element-specific bond lengths

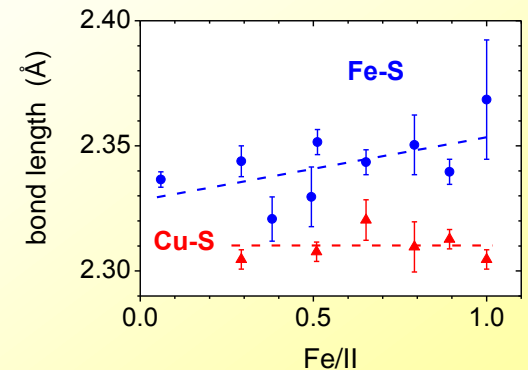
- similarities but also differences to chalcopyrite materials for $\text{Cu}_2(\text{Zn,Fe})\text{SnS}_4$



Just et al., APL 99, 2011

Zillner et al., APL 102, 2013

Zalewski et al., JAC 492, 2010



Thank you !

